NASA CR-72435

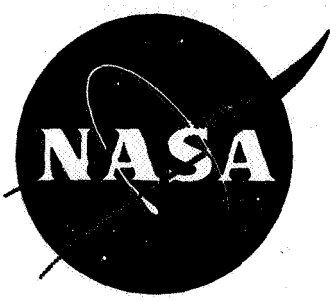

RESONANT SYSTEMS FOR DYNAMIC TRANSDUCER EVALUATIONS

by

R. E. Robinson and C. Y. Liu

Prepared for

NATIONAL AERONAUTICS AND SPACE ADMINISTRATION

CONTRACT NASr-100(08)

BATTELLE MEMORIAL INSTITUTE
COLUMBUS LABORATORIES

Requests for copies of this report should be referred to:

National Aeronautics and Space Administration
Office of Scientific and Technical Information
Washington 25, D.C.
Attention: AFSS-A

NASA CR 72435

FINAL REPORT

RESONANT SYSTEMS FOR DYNAMIC TRANSDUCER EVALUATIONS

by

R. E. Robinson and C. Y. Liu

Prepared for

NATIONAL AERONAUTICS AND SPACE ADMINISTRATION

August 31, 1968

Contract NASr-100(08)

Technical Management
NASA Lewis Research Center
Cleveland, Ohio
Marshall C. Burrows

BATTELLE MEMORIAL INSTITUTE
Columbus Laboratories
505 King Avenue
Columbus, Ohio 43201

TABLE OF CONTENTS

LIST OF TABLES

LIST OF FIGURES

LIST OF FIGURES (Cont'd)

RESONANT SYSTEMS FOR DYNAMIC TRANSDUCER EVALUATIONS

by

R. E. Robinson and C. Y. Liu

ABSTRACT

A study of methods for generating large-amplitude, high frequency dynamic pressures at high static pressures such as those encountered in rocket motor combustion instability studies was performed. Then an analytical and experimental program was undertaken to evaluate the most promising concept--an inlet-modulated, gas throttled device (siren type)--for pressure transducer evaluations.

This report describes the research conducted and the results obtained during this effort. The program was performed under contract with the U. S. National Aeronautics and Space Administration during the period March 1, 1967 to February 29, 1968.

ACKNOWLEDGMENT

During the course of the program, several Battelle professional staff members have taken part, including J. L. Harp who performed the experimental studies. The background skills and contributions of each are gratefully acknowledged.

RESONANT SYSTEMS FOR DYNAMIC TRANSDUCER EVALUATIONS

by

R. E. Robinson and C. Y. Liu

SUMMARY

Analytical studies of methods for generating large-amplitude, high-frequency dynamic pressures at high static pressures such as those encountered in rocket motor combustion instability studies were performed. During these studies, it was found that an inlet-modulated flow-through sinusoidal pressure generator showed more potential than the proposed resonant free piston oscillator with a displacement amplified piezoelectric vibrator as a driver. As a result, the experimental phase of the program was redirected.

Analytical and experimental efforts were directed to determine the feasibility, applicability, and attainable performance of such a device for pressure transducer evaluations at large-amplitude, high-frequency, and high average pressures. Also as part of the redirection, an investigation was made to determine the possible use of a NASA owned outlet-modulated sinusoidal pressure generator located at Battelle to explore the inlet-modulated concept. The investigation indicated that the available generator could be temporarily modified with no permanent effects and serve as a valid test device for most of the inlet-modulated concepts.

A series of performance tests were first made on the available outlet-modulated sinusoidal pressure generator. The testing was done to provide performance data at the same pressure and frequency conditions that the inlet-modulated testing was conducted at. The data served as a reference to determine performance improvements of the inlet-modulated concept and provided design information for the new concept. Fifty inlet-modulated sinusoidal pressure generator tests were conducted and established the concept as feasible and applicable to transducer evaluation, and also attained the performance predicted for it.

INTRODUCTION

The National Aeronautics and Space Administration has funded the research and development of transient pressure measurements and calibration or evaluation techniques and equipment over the last seven years. The work was originated at Princeton University. The technology and equipment developed there was transferred to Battelle in 1965. One of the intents for the use of this NASA equipment at Battelle was that transient pressure transducer evaluations would be performed for NASA and for other

Government agencies, their contractors and industry on a cost type research contract. This report covers work aimed at extending the pressure transducer evaluation capability.

The foundation for using a transducer as a measuring instrument lies in the assumption that within a certain range of operation, the transducer itself behaves as a linear-vibratory system. If this were not true, either the exact functional dependence of the transducer characteristics on displacement and velocity would have to be known, or the calibration environment would have to be an exact duplicate of the phenomenon to be investigated. Neither of these approaches is attainable in practice.

For a linear-oscillatory system, the only pertinent parameter is the amplitude (or magnification factor) dependence on frequency. Thus, the purpose of a transducer-calibration device is to provide an environment where such amplitude-frequency response can be obtained. Theoretically, any well-defined environmental variation such as a step or sawtooth type will be sufficient for this purpose. In practice, one such well-defined variation that can be obtained is with a shock tube. The subsequent harmonic analysis entailed in this approach makes the method cumbersome. Further, the shock tube is limited as to the amount of energy it can put into each vibrational mode. Unless the shock tube is extremely versatile, the transducer may not be sufficiently excited in the various modes which affect model inadequacies and nonlinearities associated with high frequencies, or it may be over pressured. A shock tube for higher pressures is expensive in both facility and operational costs (large amounts of light gas). The simplest means of calibrating a linear transducer is to impose a sinusoidal input. A sinusoidal generator permits a direct calibration of the transducer at the frequencies of interest without the need of sorting out undesirable parts of the signal through harmonic analysis.

Evaluation or calibration at pressure conditions corresponding to those to be measured is necessary either for absolute calibration (which assumes a response model and its associated differential equations and then determines their coefficients) or comparative calibration (which directly compares output from the transducer being calibrated with output from a standard transducer). Calibration of either type is necessary at the use pressure conditions. A mechanical model may be satisfactory at presently available calibration conditions, but inadequate at actual use conditions, or since the transducer itself may become nonlinear under the severe actual environment. That is, evaluations or calibrations made at the available low pressure-amplitude levels may be inaccurate at the more severe actual use conditions because the transducer response may change from linear to nonlinear, or the assumed mechanical response model may no longer be adequate.

No sinusoidal pressure generators, SPG's, were available for evaluation of pressure transducers at conditions closely similar to the large-amplitude, high-frequency oscillations at high average pressures of unstable rocket motors. The original objectives of the present work were:

I. To provide analytical and experimental effort directed toward the development of a resonant free-piston oscillator with a displacement-amplified piezoelectric vibrator as a driver. To determine the feasibility, applicability and attainable performance of such a device for pressure transducer evaluations at large-amplitude, high-frequency and high average pressures.

II. To develop a primitive system which will demonstrate and evaluate such a system for evaluating pressure transducers.

III. To explore other resonant concepts which might be used in achieving high-amplitude oscillations.

Resonant systems were initially chosen because the oscillation amplitude in many systems may be significantly increased by operating the environmental system at resonance, which occurs at specific frequencies or limited bands of frequencies. The large-amplitude oscillations, at the system natural or resonant frequency, occur only after a few cycles of operation. During this time, the energy of the forcing function is being stored in the system--producing oscillations of increasing amplitude. The process continues until the system damping balances the input by the forcing function. The system continues to oscillate at the largest amplitude achieved during the buildup or energy-storage procedure and the energy input from the forcing function is dissipated by the damping. A resonant system thus allows oscillations at large amplitudes without requiring a power source or forcing function capable of putting the large-amplitude energy into the system on each cycle--the forcing function must only match the damping force.

A resonant free-piston is a device employing this principle. Basically, the device consists of two pistons in a gas-filled cylinder. One piston is located near a closed end of the cylinder and is free to oscillate between upper and lower limit stops. The other piston is located near the other end of the cylinder and is connected to an oscillating power source. The gas in the chambers formed by the pistons behaves as springs. When the driven piston is oscillated at a resonant frequency of the system, the oscillation amplitude of the free piston is greater than that of the driver piston. Thus, large amplitudes may be obtained from smaller oscillation amplitudes than are available with realistic drivers. A transducer mounted in the closed end could thus be exposed to high-amplitude oscillatory pressures by attaining a free-piston displacement of the order of the length between the mean piston position and the closed end. A displacement-amplified, resonant, magnetostrictive transducer or piezoelectric vibrator was selected for a driver.

At the beginning of the contract period, several new concepts for generating large-amplitude dynamic pressures were being advanced. These concepts were:

- A strong travelling traverse acoustic mode concept being developed at NASA-Lewis by Mr. M. F. Heidmann.

- A Battelle concept based on a flow inlet-modulated, gas-throttled device (siren type).

Consequently, the third part of the program objectives, the exploration of other resonant concepts, including the above two concepts, was performed first. The pertinent conclusions from this study were:

(1) That the acoustic resonators can produce sinusoidal pressure variations at low frequencies (<1,000 cps) and low biased pressures (around atmospheric). At higher frequencies and pressures, the pressure wave degenerates into more or less sawtooth form.

(2) That the fixed-mass, variable-volume generators are convenient calibrators for low frequencies (~2,000 cps) or for low amplitude (<1 percent of static pressure) at high frequencies (~10,000 cps). It is possible to increase the amplitude by developing energetic but costly drivers such as a piezoelectric or magnetostrictive resonance element. However, because of material-strength limitations, it is nearly impossible to construct a driver to produce a 10 percent peak-to-peak dynamic pressure/static pressure (based on a 0.01-inch-total driver displacement on a 0.1-inch gap for the fluid cavity) at 10,000 cps even though the pressure variation may be sawtooth in form.

(3) That the present outlet-modulated SPG is capable of creating large-amplitude pressure variations at a wide frequency spectrum (a minimum of 5 percent peak-to-peak dynamic pressure/static pressure over the range of 50 to 10,000 cps.

(4) Theoretical calculation predicts that with inlet-flow modulation both the amplitude and frequency range of a gas throttled SPG can be increased. Furthermore, the pressure variation always remains sinusoidal since there is no higher harmonic excitation existing in this system as in all the other systems examined.

Consequently, the inlet-modulated SPG concept was selected for further investigation by actually building a system for preliminary tests. This was to be done by using the existing NASA SPG at Battelle with the necessary modification of converting the outlet to inlet modulation if possible. The first two original objectives of the program were replaced with:

I. Analytical and experimental effort directed toward the development of a flow-through, inlet-modulated sinusoidal pressure generator. To determine the feasibility, applicability, and attainable performance of such a device for pressure transducer evaluations at large-amplitude, high-frequency, and high-average pressures.

This report discusses the analytical study performed of the various concepts and the analytical and experimental studies performed to evaluate the inlet-modulated sinusoidal pressure generator concept.

EVALUATION OF CONCEPTS

A critical examination was conducted of the major existing sinusoidal transducer calibration techniques and of the new calibration concepts advanced. Notable among the latter are the acoustic transverse wave generator conceived at NASA-Lewis, the inlet-flow-modulating sinusoidal pressure generator suggested by Battelle, and the double-piston generator discussed in the original proposal of the present contract. The evaluations are concerned with performance characteristics such as amplitude, frequency, harmonic distortion, and biased pressure level. For convenience in evaluation, the generators can be classified according to the physical mechanisms used to produce the pressure variation into:

(1) Acoustic resonator

- (a) Siren-tuned cavity generator
- (b) Piston-in-cylinder generator
- (c) Transverse-wave generator

(2) Fixed-mass, variable-volume generator

- (a) Piston-in-cylinder generator
- (b) Double piezoelectric crystal generator
- (c) Double-piston generator

(3) Variable-mass, fixed-volume generator

- (a) Outlet-modulated generator
- (b) Inlet-modulated generator

Acoustic Resonators

For this type of generator, the primary mechanism to cause a pressure variation in a fluid cavity is the acoustic wave produced by an excitation source. In the siren-tuned cavity generators in Figure 1 and

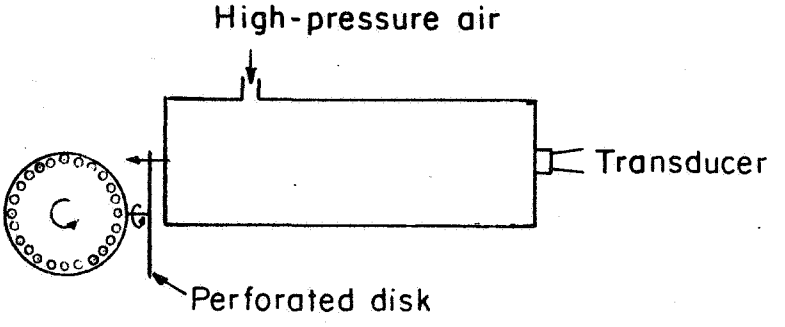

FIGURE 1. SIREN-TUNED-CAVITY GENERATOR.

in the piston-in-cylinder generator in Figure 2, the fundamental mode

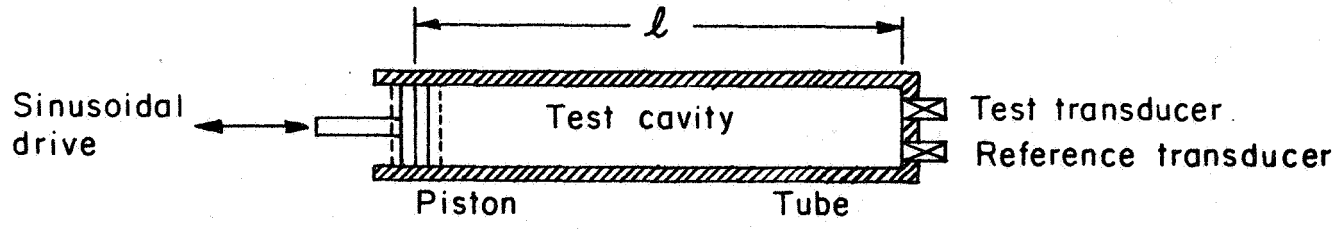

FIGURE 2. PISTON-IN-CYLINDER GENERATOR.

excited is the longitudinal wave along the cylinder axis. In Figure 1, the excitation source is through the interruption of gas flow by means of a perforated rotating disc. In Figure 2, the excitation can be produced by either an oscillating piston or a piezoelectric stack. To produce resonance in the cavity, the cylinder length has to be a multiple of the acoustic half-wave length. This means that, in an actual calibration device for different frequencies, either the cavity length is adjustable or different length cylinders are provided. Theoretical analysis was developed for the motion of the gaseous medium[1]* and for the formation and behavior of shock waves generated by the coalescence of compression waves[2]. In actual operation, the gas motion is more complicated than the simplified model used in the theory and at resonance frequency, the pressure waves are always distorted from the sinusoidal excitation motion. In siren-tuned generators, repetitive sawtooth pressure waves can be achieved at frequencies from 50 to 1000 cps, and for the piston-in-cylinder generator, clean sinusoidal waves are possible for frequencies less than 500 cps[3].

Recently, M. F. Heidmann of NASA-Lewis[4] proposed a generator using a very short cylindrical cavity with a rotating gas jet at the cylinder axis as shown in Figure 3. The thinness of the cylinder prevents exciting the longitudinal wave. Preliminary tests have shown that at a jet gas pressure of 62.5 psia, a reasonably clean sinusoidal pressure wave is obtained for frequencies less than 700 cps and maximum peak-to-peak amplitude of 2.5 psi. At higher jet pressures, the wave changes to an approximate sawtooth form. The governing equations are the conservations of mass and momentum, represented by

$$\frac{\partial \rho}{\partial t} + \rho \ \text{div}\ V + V \cdot \text{grad}\ \rho = 0$$

$$\frac{\partial V}{\partial t} + (V \cdot \text{grad})\ V = -\frac{1}{\rho}\ \text{grad}\ p \quad ,$$

* Numbers in parentheses refer to references listed at the end of this report.

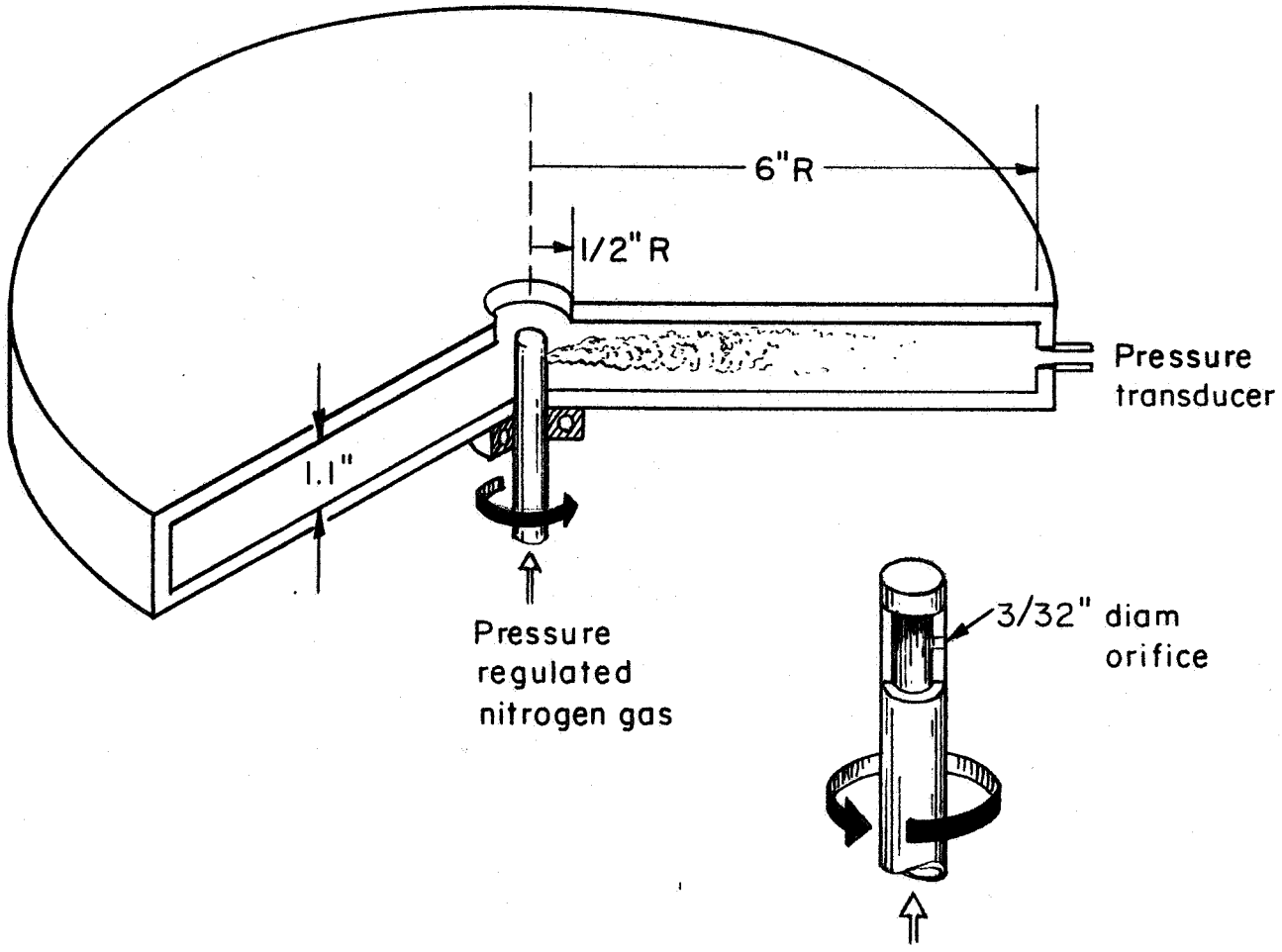

FIGURE 3. TRANSVERSE ACOUSTIC WAVE GENERATOR.

where V is the velocity vector, ρ is the fluid density, and p is the pressure. Introducing the velocity potential φ, defined by

$$V = \text{grad } \varphi \quad ,$$

the governing equations become

$$\frac{\partial \rho}{\partial t} + \rho \nabla^2 \varphi + V \cdot \text{grad } \rho = 0$$

$$\text{grad } \left(\frac{\partial \varphi}{\partial t} + \frac{1}{2} V^2 + \frac{p}{\rho} = 0 \right) \quad .$$

Thus, for a small quasi-steady variation, the pressure is measured relative to an average value of $\bar{p}$ and the convection term $\frac{1}{2} V^2$ may be neglected to give

$$p = \bar{p} - \rho \frac{\partial \varphi}{\partial t} \quad .$$

Furthermore, if the process is isentropic, the sonic velocity C is

$$C^2 = \frac{\partial p}{\partial \rho}$$

or

$$\delta \rho = \frac{1}{C^2} \delta p = - \frac{\rho}{C^2} \frac{\partial \varphi}{\partial t} \quad .$$

In the continuity equation, dropping the higher order term $V \cdot \text{grad } \rho$ and writing $\frac{\partial \rho}{\partial t} = - \frac{\rho}{C^2} \frac{\partial^2 \varphi}{\partial t^2}$ for small density change, this results in

$$\nabla^2 \varphi = \frac{1}{C^2} \frac{\partial^2 \varphi}{\partial t^2} \quad .$$

From the above equation, the transverse wave in a circular cavity of radius, a, is given by

$$\varphi = A_n J_n \left(\frac{\omega}{c} a\right) \sin (\omega t + n\theta) \quad ,$$

where A_n is an arbitrary constant, J_n is the Bessel function of order n, ω is the travelling wave frequency, and θ is the angular position. The pressure is then

$$p = \bar{p} \left[1 - \frac{\rho \omega A_n}{\bar{p}} J_n \left(\frac{\omega}{c} a\right) \sin (\omega t + n\theta)\right] \quad .$$

Heidmann's preliminary test shows that the oscillation excited by the revolving gas jet is this transverse mode in the cavity. It is apparent from the above expressions that to excite the fundamental mode at different frequencies, cavities of different radii would have to be used. At the high jet pressures and/or frequencies of interest here, the above linearized theory is inadequate. This inadequacy results because the fluid inertia effect becomes important and/or the process can no longer be considered isentropic. That fluid friction may also become important was not taken into account in the above theoretical derivations. Consequently, more detailed theoretical analysis than has already been performed by Heidmann does not appear to be warranted. The limits on the usefulness of the acoustic-wave generator for transducer calibration must be determined by experiment.

Fixed-Mass, Variable-Volume Generators

Instead of using the acoustic wave in a large cavity, this group of generators employs very thin cylindrical cavities to suppress the longitudinal acoustic oscillation while using the compressibility property of the fluid as the mechanism to produce pressure variation. The difference among generators is the excitation source. Typical among them are the piston-in-cylinder generator shown in Figure 4, double-crystal generator shown in Figure 5, and acoustic-coupled double-piston generator shown in Figure 6. The problems for this type of generator come from two sources: the fluid cavity and the driver.

Governing Equations

For an ideal generator of gap size ℓ_o and equilibrium pressure p_o, an isentropic compression of a gas is given by

$$p\ell^\gamma = p_o \ell_o^{\ \gamma} \quad ,$$

where p is the instantaneous pressure, ℓ is the gap size, and γ is the ratio of specific heats. If the driver causes ℓ to change according to

$$\ell = \ell_o (1 + \alpha \sin \omega t) \quad ,$$

where α is the percent amplitude based on ℓ_o, the pressure and the percent dynamic pressure are

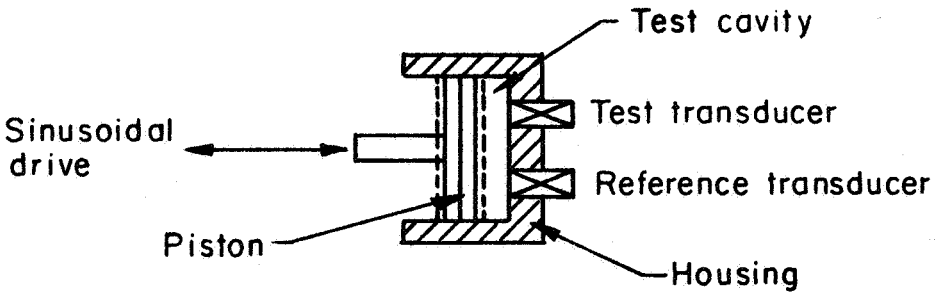

FIGURE 4. PISTON-IN-CYLINDER GENERATOR.

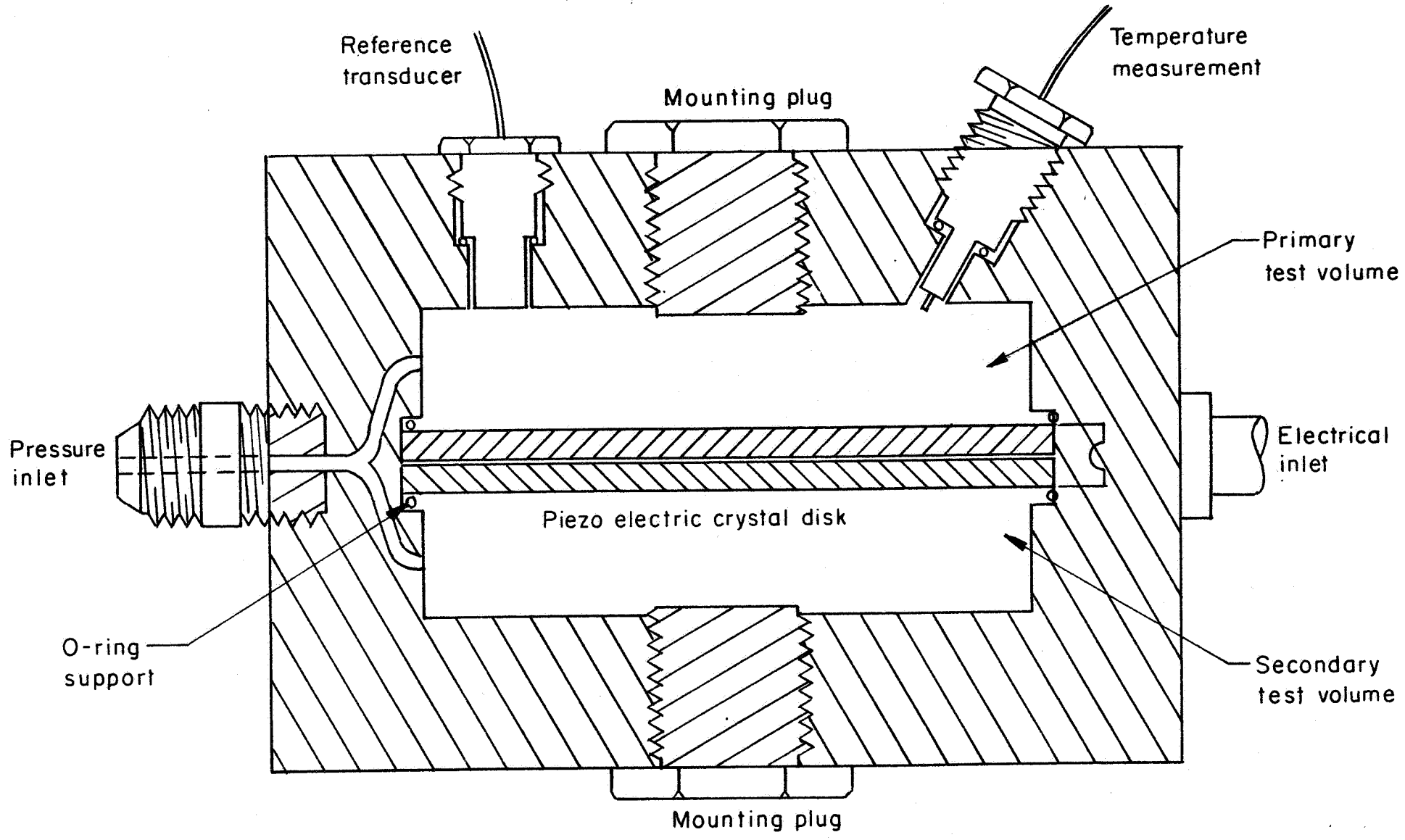

FIGURE 5. SCHEMATIC OF DOUBLE-CRYSTAL PRESSURE GENERATOR.

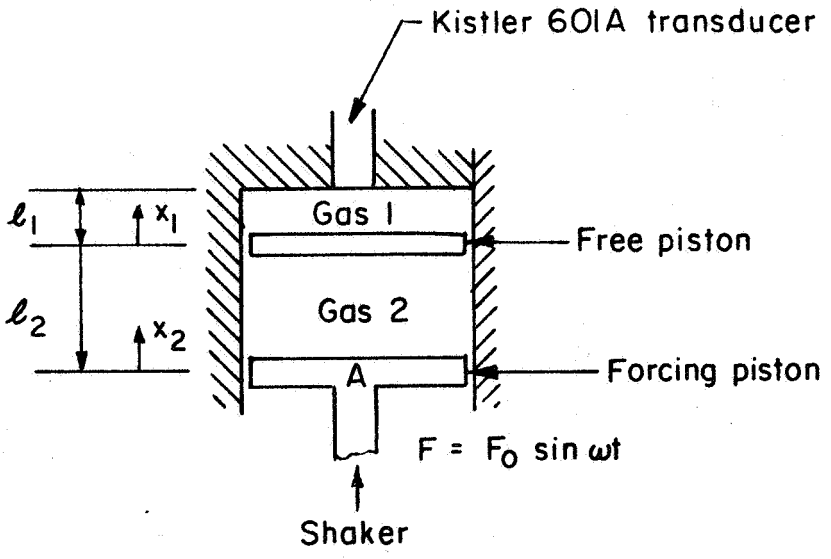

FIGURE 6. DOUBLE-PISTON GENERATOR

$$p = p_o (1 + \alpha \sin \omega t)^{-\gamma}$$

$$\frac{p_o - p}{p_o} = 1 - (1 + \alpha \sin \omega t)^{-\gamma} = \alpha \gamma \sin \omega t - \frac{\alpha^2}{2} \gamma (\gamma + 1) \sin^2 \omega t \ldots ,$$

where terms beyond the first represent higher harmonics. For small values of the higher harmonics,

$$\frac{p_o - p}{p_o} \simeq \alpha \gamma \sin \omega t \quad .$$

For α = 4 percent, the maximum amplitude $(p_o - p)/p_o$ = 5.6 percent (γ = 1.4), 6.64 percent (γ = 1.66), and the harmonic distortion defined as $\alpha\gamma - [1-(1+\alpha)^{-\gamma}]/\alpha\gamma$ = 4.65 percent (γ = 1.4), 5.13 percent (γ = 1.66). To gain amplitude, the percent driver amplitude must be large. Since most driver displacements at high frequency are limited, the cavity gap size must be extremely small. This simplified theory does not take into account influences due to fluid motion and viscous effect.

Though the acoustic wave in the longitudinal direction can usually be suppressed, to accommodate the transducers to be calibrated, a reasonable dimension must be provided in the diametrical direction where transverse and radial waves can be produced. For example, an air cavity of 1-inch diameter has a fundamental resonance frequency of about 3400 cps. Near resonance condition, not only harmonic distortion becomes large, but also the pressure in the cavity is no longer uniform.

It is intuitively apparent that a large-displacement, high-frequency driver entails large acceleration and deceleration and large energy dissipation. Various means have been attempted to achieve these requirements. Morefield(5) used a hydraulic actuator to drive a piston as in Figure 4. Using liquid oil in the cavity, he obtained a peak-to-peak pressure of 40 psi at 2000 cps with a biased pressure of 5000 psi. Fluid leakage around the piston or seals for its prevention can cause both a reduction of the amplitude and distortion of the pressure variation.

Piezoelectric Crystal Generators

Considerable effort has been expended to develop piezoelectric driven generators and a number of designs are available. This utilizes the piezoelectric property of a material; i.e., strains and stresses are developed in the material when an electric field is applied. The driver designs are usually of two types; the series stack where a number of thin discs are cemented together and connected electrically in parallel, the

other type is the double crystal or bi-morph design which has two crystals arranged such that one crystal expands while the other contracts thereby providing a bending mode. The double crystal design has been used most frequently and is shown in Figure 5. The advantages of the arrangement in Figure 5 are that relatively smaller cavity diameters can be used for comparison calibration and very high driver frequency is easily attainable. However, the ultimate strain of the material is usually very small, severely limiting the dynamic pressure variation obtainable (less than 1 percent of the biased pressure at 10 kcs). Heating of the material from hysteresis loss also limits the frequency obtainable.

Possible performance obtainable from a crystal-driven type sinusoidal pressure generator is difficult to determine because of the many design concepts and materials available. Some minimum requirements from consideration of the gas media behavior can, however, be defined.

Considering a double cavity design similar to that of Figure 5, two types of phenomena may be used to generate pressure variations in the cavities, a wave or acoustic phenomenon, or a compression phenomenon. Pressure conditions of 100 psi peak-to-peak at 15,000 hertz and 30 psi at 35,000 hertz, both at a static or mean pressure of 2,000 psia are investigated.

The wave length of these two frequencies in helium and nitrogen are determined from $\frac{c}{f}$ as:

f	λ_{He}	λ_{N2}
15,000	3.03 inches	0.922 inch
35,000	1.3 inches	0.395 inch

Thus, the length of the cavity must be of the order of several inches for the frequency range to operate in the acoustic mode and, or course, much larger at the lower frequencies.

The power per unit area that must be supplied to the gas in one cavity to achieve the aforementioned acoustic mode pressure oscillations for helium and nitrogen are determined from:

$$p = \rho\ c\ \omega\ A \text{ and } I = \frac{1}{4}\rho\ c\ \omega^2\ A^2 \quad ,$$

as

p, psi	$\omega/2\pi$, hertz	A_{He}, in.	A_{N2}, in.	I_{He}, kw/in.^{2}	I_{N2}, kw/in.^{2}
50	15,000	0.00656	0.00259	0.875	0.342
15	35,000	0.00084	0.00033	0.078	0.031

The ideal power required for a perfect double cavity device using a 4-inch diameter crystal having an area = 0.7854 x 16 = 12.6 $in.^2$ is

p, psi	$Power_{He}$, kw	$Power_{N2}$, kw
50	22.0	8.6
15	1.96	0.78

The simplified analyses governing equations for the compression mode are given on Page 16. For the two study conditions, the following relationships are found

$$\frac{p_o - p}{p_o} = \alpha\ \gamma = \begin{cases} \frac{50}{2000} = 0.025 \\ \frac{15}{2000} = 0.075 \end{cases}$$

$$\Delta\ell = \ell_o - \ell = \begin{cases} \frac{0.025}{\gamma}\ \ell_o \\ \frac{0.0075}{\gamma}\ \ell_o \end{cases}$$

It is difficult to estimate the power required for a compressive-type oscillator. For example, in a perfect or ideal device, there would be no power required to sustain the oscillation once it was in motion. The power per unit area to start the motion for one side may be estimated from

$$\text{Power/area/side/}_{\text{adiabatic}} = \left(\frac{\gamma}{\gamma - 1}\right) \frac{2\ p_o \ell_o\ f \times 60}{12 \times 44.27 \times 10^3} \left[\left(\frac{p}{p_o}\right)^{\frac{\gamma-1}{\gamma}} - 1\right]_{kw/in.^2}$$

For the previous conditions

p, psi	f, hertz	I_{He}, $kw/in.^2$	I_{N2}, $kw/in.^2$
50	15,000	170 ℓ_o	169 ℓ_o
15	35,000	211 ℓ_o	210 ℓ_o

Considering an oscillator capable of producing a displacement, $\Delta\ell$, of the order of magnitude of that required for the acoustic mode, say, 0.0005 inch at 35,000 hertz, the associated cavity length, ℓ_o for helium would be

$$\ell_o = \frac{\Delta \ell \gamma}{0.0075} = \frac{0.0005 \times 1.66}{0.0075} = 0.11 \text{ in.}$$

The power per unit area required for both sides is

$$\text{Power/area} = 2 \times 210 \times 0.11 = 46.2 \text{ kw/in.}^2$$

The power for a 4-inch diameter crystal at these conditions would be 581 kw. Obviously, a device would not have to deliver anywhere near this power except for a very small fraction of a second. The actual running power will depend upon the design crystal vibrational mode, material (hysteresis effects), gas leaks, and compressive losses. Though efficiencies for crystal transducer may reach 50 percent for a very specific and narrow frequency band, the usual efficiencies are 10 percent and below. Thus, the power requirements to the crystal driver will be increased by about an order of magnitude over that required in the gas.

Another point of consideration is the voltage requirements. For the frequently used x-cut quartz crystal in a thin plate design, the voltage may be estimated from

$$p = \rho c \omega A = \epsilon_{xx} \frac{E_o}{T_x} ,$$

where ϵ_{xx} is the piezoelectric stress coefficient = 0.17 coulomb/meter^2 for an x-cut quartz crystal, T_x is the crystal thickness, and ρc is the crystal impedance = 1.5 x 10/Rayleighs. The voltage is then expressed as

$$E_o = 3.87 \times 10^{13} A T_x ,$$

where A and T_x are in the meters.

For the acoustic mode, A = 0.0033 in. = 1.3×10^{-6} meters. Maximum strains for the class of crystals needed is normally a maximum of one part in 10,000. Thus,

$$T_x = \frac{A}{10^{-4}} = 1.3 \times 10^{-2} \text{ meters}$$

The required voltage is

$$E_o = 3.87 \times 10^{13} A \left(\frac{A}{10^{-4}}\right) = 653{,}000 \text{ volts}$$

This would be an extremely difficult design problem for powers in the kilowatt range.

Examination of the compression mode and reducing the voltage requirements to a still high and difficult level of 2000,000 volts and maintaining the same strain restriction gives a displacement amplitude of

$$A = \sqrt{\frac{E_o}{3.87 \times 10^{17}}} = 0.719 \times 10^{-6} \text{ meter} = 0.0000283 \text{ inch} \quad .$$

The associated cavity length required for nitrogen would be

$$\ell_o = \frac{\Delta \ell \gamma}{0.0075} = \frac{0.0000283 \times 1.4}{0.0075} = 0.0053 \text{ inch} \quad .$$

This type of design involving quartz would require a high voltage system involving very difficult dimensional tolerances. Larger dimensions would necessitate higher voltages.

In the above estimates, the influence due to reflection at the crystal-gas interface has been ignored, because it will not alter the order of magnitude of the estimations.

The complexities of trying to cover a wide range of frequencies further complicate the design and several units using either different crystals, crystal cuts, variable cavity lengths, or pressure generation phenomena may be necessary. The actual gas behavior which will have acoustic or weak shock-type waves could add additional difficulties from their reflections and interactions. Other problems not considered, but to be faced, are crystal power limitations, saturation, and heat.

In summary, a quartz crystal-driven sinusoidal pressure generator requires either a high voltage-high power design or a high-voltage design involving dimensional sensitivity. The pressure-frequency conditions considered are probably the maximum obtainable, but the lower operational cost of a nonflow-through system is attractive. A compromise design might be a resonant concept. Less power and voltage would be required at the expense of frequency-pressure conditions.

Double-Piston Generator

Preliminary tests carried out at Battelle using an acoustic piston driver as shown in Figure 6 showed that sinusoidal variation is possible for frequencies less than 500 cps. At higher frequencies, the variation degenerated into more or less sawtooth form. It is doubtful that sinusoidal variation can be obtained at very high frequency because the device possesses the disadvantage of both the short and long cavities. If the acoustic coupling can be suppressed, a first-order theory for the double-piston generator can be derived as follows.

Assuming an isentropic process in the gases and neglecting any damping, the displacements x_1 and x_2, Figure 6, are related by

$$m_1 \ddot{x}_1 = pA\left[\left(\frac{\ell_2}{\ell_2 + x_1 - x_2}\right)^{\gamma} - \left(\frac{\ell_1}{\ell_1 - x_1}\right)^{\gamma}\right]$$

$$m_2 \ddot{x}_2 = pA\left[1 - \left(\frac{\ell_2}{\ell_2 + x_1 - x_2}\right)^{\gamma}\right] + F_o \sin \omega t \quad .$$

and the pressure in the upper chamber, p_1, is related to the average pressure, p, by

$$p_1 = p\left(\frac{\ell_1}{\ell_1 - x_1}\right)^{\gamma} \quad ,$$

where A is the cylinder area, m_1 and m_2 are the masses of the pistons, γ is the ratio of specific heats, and the same gas is used in both chambers.

For small displacements, i.e., $|x_1 - x_2| \ll \ell_2$, $|x_1| \ll \ell_1$, the above relations can be approximated by

$$m_1 \ddot{x}_1 = -p\frac{A\gamma}{\ell_1}\left[\left(1 + \frac{\ell_1}{\ell_2}\right)x_1 - \frac{\ell_1}{\ell_2}x_2\right] + \frac{\gamma(\gamma+1)}{2} pA\left[\left(\frac{x_1 - x_2}{\ell_2}\right)^2 - \left(\frac{x_1}{\ell_1}\right)^2\right] - \ldots.$$

$$m_2 \ddot{x}_2 = p\frac{A\gamma}{\ell_2}\left[x_1 - x_2 - \frac{(\gamma + 1)}{2\ell_2}(x_1 - x_2)^2 + \ldots.\right] + F_o \sin \omega t$$

$$p_1 = p\left[1 + \gamma\frac{x_1}{\ell_1} + \frac{\gamma(\gamma + 1)}{2}\left(\frac{x_1}{\ell_1}\right)^2 + \ldots.\right] \quad .$$

Using only the linear terms gives the steady-state solution

$$x_1 = x_{10} \sin \omega t$$

$$x_2 = x_{20} \sin \omega t$$

$$\frac{p_1 - p}{p} = \gamma\frac{x_{10}}{\ell_1} \sin \omega t \quad ,$$

where

$$x_{10} = (F_o/K_1) \Big/ \left[\left(\frac{\omega^2}{\omega_2^2} - 1\right)\left(\frac{\omega^2}{\omega_2^2} - 1\right) - \frac{\ell_1}{\ell_2}\frac{\omega^2}{\omega_2^2}\right]$$

$$x_{20} = (F_o/K_2\left(1 + \frac{\ell_1}{\ell_2} - \frac{\omega^2}{\omega_1^2}\right) \Big/ \left[\left(\frac{\omega^2}{\omega_1^2} - 1\right)\left(\frac{\omega^2}{\omega_2^2} - 1\right) - \frac{\ell_1}{\ell_2}\frac{\omega^2}{\omega_2^2}\right]$$

$$K_1 = pA\ \gamma/\ell_1$$

$$K_2 = pA\ \gamma/\ell_2$$

$$\omega_1^2 = K_1/m_1$$

$$\omega_2^2 = K_2/m_2 \quad .$$

Resonance will occur when the denominators in the expressions for x_{10} and x_{20} vanish. However, the linearized sinusoidal solutions will no longer hold. A second approximate solution is

$$x_1 = x_{10}\left[\sin \omega t + \left(\frac{\gamma + 1}{16}\right)\left(\frac{\omega^2}{\omega_1^2} - 2\right)\frac{x_{10}}{\ell_1}\cos 2\ \omega t\right]$$

$$\frac{p_1 - p}{p} = \frac{\gamma x_{10}}{\ell_1}\left[\sin \omega t + \left(\frac{\gamma + 1}{16}\right)\left(\frac{\omega^2}{\omega_1^2} - 6\right)\frac{x_{10}}{\ell_1}\cos 2\ \omega t\right] \quad .$$

Thus, the harmonic distortion increases at resonance or at large amplitude, even if an energetic driver is used.

The development of an energetic, high-frequency, large-displacement driver is required to explore fixed-mass systems.

Sonic generators consisting of a tapered solid horn or stepped solid horns driven in longitudinal resonance by piezoelectric or magnetostrictive elements are essentially single-frequency generators. The tapered or the stepped horns are used to obtain an amplification of the displacement obtained at resonance from the output end of the driving elements. The "sharpness" of the resonance curve and the peak displacement are functions of the mechanical Q, i.e., the ratio of energy stored in the vibratory system to energy dissipated.

The bandwidth of the system is also a function of the Q (inversely proportioned to the Q). Thus, to obtain a bandwidth to include frequencies from 40 cps to 15 kcps would require a Q approaching 1, but this is in opposition to obtaining large displacements.

The range of frequencies can be obtained by using multiple units--a separate transducer (ultrasonic generator) for each frequency. Longitudinally resonant systems could be used at higher frequencies but other modes such as flexural resonances would be necessary at lower frequencies; otherwise, the size of the sonic generators would become prohibitively large.

A total displacement in the order of 0.010 inch without damage to the generator system at frequencies from 10 kcps to 15 kcps are nearly impossible in a resonant system. For instance, the maximum stress developed in a halfwave, longitudinally resonant, uniform bar of stainless steel at 10 kcps is approximately 45,000 psi, if the total displacement at the end is 0.010 inch (0.005-inch displacement amplitude). This stress occurs halfway between the two ends of the bar or at the velocity node. If this displacement is accomplished by a stepped-horn configuration (two cylinders of different diameter, but each a quarter-wavelength long and having a common axis), the step occurs at the point of maximum stress and, therefore, the maximum stress is increased by a factor which is a function of the fillet radius.

An estimate of the power required to obtain 0.010-inch total displacement at the end of a longitudinally resonant solid horn at 10 kcps is 10 kw, if the radiating surface is 1 inch in diameter.

Variable-Mass, Fixed-Volume Generators

Structurally, this type of generator can be viewed as a modification of the siren-tuned cavities described previously. A very thin cylindrical cavity is used to suppress the longitudinal acoustic waves. Critical flow orifices are used at both the gas inlet and outlet openings as shown in Figure 7. A perforated rotating disc at either the inlet or outlet makes it possible to vary the amount of gas remaining in the cavity at any instant and thus to create a pressure variation. The outlet-modulated sinusoidal pressure generator was developed at Princeton University under various NASA contracts. The Princeton-developed generator is currently operated at Battelle's Columbus Laboratories as part of the facilities of the Transducer Evaluation Laboratory for NASA. The theoretical background for this SPG is given in detail in the next section. Battelle suggested the possibility of improving the quality of such an SPG by means of an inlet-modulated gas flow. A preliminary theoretical study was made. The detailed results of this study are also given in the next section. The flow-modulated generators have the following advantages: (1) the fluid flow has a fast response at high flow rates so that large amplitudes are obtainable at high frequencies and (2) the two flat side surfaces of the small cavity allow a comparison test of two transducers so that satisfactory high-frequency conditions can be obtained. The disadvantage of this type of generator is the operation cost involved with providing high-pressure gas and with losing it to the surroundings after flow through the cavity.

The present SPG has been operated at a biased pressure of 250 psi, giving a reasonably clean sinusoidal peak-to-peak dynamic pressure of 12 psi at 10,000 cps. At higher frequencies, the wave shape becomes distorted

from a sinusoidal variation. Theoretically, the inlet-modulated SPG would reduce greatly the harmonic distortion. Until an actual unit is constructed, this improvement remains conceptual.

Governing Equations of Flow-Modulated SPG

The flow-modulated SPG is generally designed on the following conditions: (1) modulating frequency is below system resonance frequency and (2) the flows through the modulating orifices are at critical flow condition. Condition (1) means that pressure variation in the gas produced by the modulation will be quickly transmitted to the entire gas by the high-speed acoustic wave so that the gas condition can be treated as a uniform medium at any instant. This makes it possible to analyze the SPG by using the gas flow relation while the detailed wave propagation in the gas can be ignored. Condition (2) results in controllable modulation with no interaction between modulating flow and downstream pressure.

Based on the above two conditions, an SPG as shown in Figure 7 can be analyzed as follows.

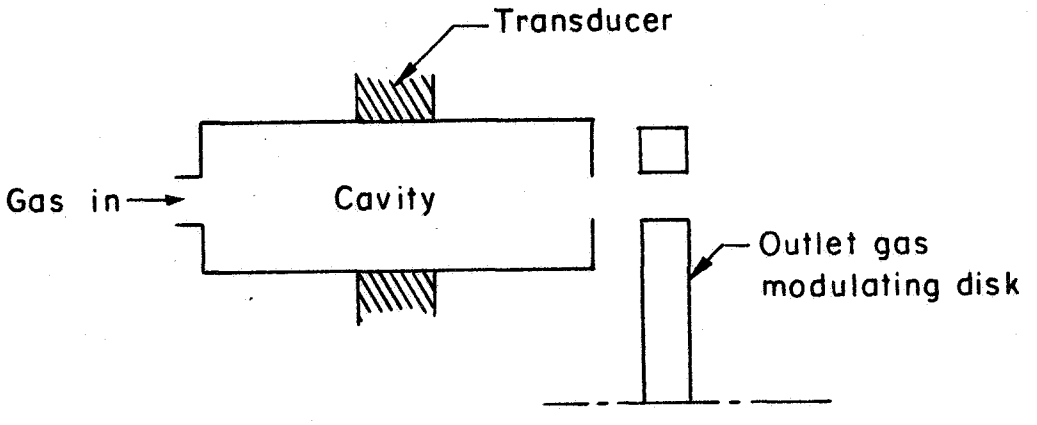

FIGURE 7. OUTLET MODULATED SINUSOIDAL PRESSURE GENERATOR.

From conservation of mass, the time rate of mass increase in the chamber $\dot{m}$ is related to the inlet flow rate $\dot{m}_{in}$ and outgoing flow rate m_{out} by

$$\dot{m} = \dot{m}_{in} - \dot{m}_{out} \quad .$$

For perfect gas at critical flow

$$\dot{m}_{in} = \alpha A_i p_o$$

$$\dot{m}_{out} = \alpha A_e p$$

$$\dot{m} = \frac{V}{RT_o} \dot{p}$$

$$\alpha^2 = \frac{g_c \gamma}{RT_o} \left(\frac{2}{\gamma + 1}\right)^{(\gamma + 1)/(\gamma - 1)}, \text{ a constant,}$$

where A_i = inlet throat area, A_e = exit throat area, p_o = stagnation pressure of supply gas, T_o = stagnation temperature of supply gas, p = chamber pressure, V = chamber volume, R = gas constant, γ = ratio of specific heats, and g_c = unit conversion factor = 32.17 lb_f - ft/lb_m - sec^2.

Combining the above relations yields

$$\dot{p} = \frac{\alpha RT_o}{V} (A_i p_o - A_e p)$$

or

$$\frac{\dot{p}}{p_o} = \eta \left(A_i - A_e \frac{p}{p_o}\right) , \tag{1}$$

where

$$\eta = \frac{\alpha RT_o}{V} = \frac{C}{V} \left(\frac{2}{\gamma + 1}\right)^{(\gamma + 1)/2(\gamma - 1)} , \text{ a constant} \tag{2}$$

$$C = (g_c \gamma RT_o)^{\frac{1}{2}}, \text{ sonic velocity at gas supply.}$$

Denoting $p/p_o = p^*$, Equation (1) becomes

$$\dot{p}^* = \eta (A_i - A_e p^*) . \tag{3}$$

Equation (3) is the governing equation for an ideal SPG. The modulation of pressure can be achieved by varying the exit area A_e and/or the inlet area A_i. The existing SPG operated at Battelle for NASA is equipped with an outlet-modulation device. From Equation (3), it is seen that exit modulation causes interaction with the pressure response because of the term $A_e p^*$. This will be discussed in detail next.

Outlet-Modulated SPG

Take a modulating area

$$A_e = \frac{A_{em}}{2} (1 + \cos \omega t) \quad ,$$

where A_{em} is the maximum opening, ω is the frequency, and t is time. Equation (3) becomes

$$\dot{p}^* = \eta \left[A_i - \frac{A_{em}}{2} (1 + \cos \omega t)\, p^*\right] \quad . \tag{4}$$

Equation (4) shows that the pressure variation p^* in general is not simple harmonic though the equation is linear. Now, if it is assumed that the variation takes place around an average pressure $\bar{p}$ which is time dependent and

$$p^* = \bar{p} + \tilde{p} \quad , \tag{5}$$

where $\tilde{p}$ is the oscillatory part of the pressure, Equation (4) becomes

$$\dot{\tilde{p}} = \eta \left[\left(A_i - \frac{A_{em}}{2} \bar{p}\right) - \frac{A_{em}}{2} \bar{p} \cos \omega t - \frac{A_{em}}{2} \tilde{p} (1 + \cos \omega t) \right] \quad . \tag{6}$$

It is clear from Equation (6) that simple harmonic response

$$\tilde{p} = - (\eta A_{em} \bar{p}/2 \omega) \sin \omega t \tag{7}$$

is possible only when the first and third terms on the right-hand side of Equation (6) vanish or are small comparing with the second term, i.e.,

$$\bar{p} = 2 A_i / A_{em} \tag{8}$$

$$\tilde{p}/\bar{p} \leq \frac{\eta A_{em}}{2 \omega} << 1 \quad . \tag{9}$$

Equation (8) defines the average pressure while Equation (9) imposes limitations on the performance of an SPG. To see clearly these limitations, a second-order solution of Equation (6) is derived by substituting Equations (7) and (8) into the right of Equation (6)

$$\dot{\tilde{p}} = -(\eta A_{em}\bar{p}/2)\left[\cos \omega t - (\eta A_{em}/2\omega)(\sin \omega t + 1/2 \sin 2\omega t)\right]$$

Integrating and taking the integration constant to be zero to ensure periodic motion gives

$$\tilde{p} = -(\eta A_{em}\bar{p}/2\omega)\left[\sin \omega t + (\eta A_{em}/2\omega)(\cos \omega t + 1/4 \cos 2\omega t)\right] \quad . \tag{10}$$

Thus, phase shift and higher harmonics will appear if Equation (9) is not true.

It is clear that because of the interaction between the modulating flow and the pressure response, an exit-modulated SPG is ideally satisfactory only for low amplitude and from Equation (7) the amplitude diminishes as the frequency increases (see Figure 8).

Inlet-Modulated SPG

To avoid the complications from exit modulation, it is necessary to keep the exit area A_e constant. The alternative approach is to vary the inlet area A_i. Now let us proceed formally by introducing Equation (5) into Equation (3),

$$\dot{\tilde{p}} + \eta A_e \tilde{p} = \eta (A_i - A_e \bar{p}) \quad . \tag{11}$$

If the inlet area is made of two openings apportioned according to the relation

$$A_i = \bar{A}_i + \tilde{A}_i \quad , \tag{12}$$

where $\tilde{A}_i$ is a variable opening and $\bar{A}_i$ is a constant opening of size $A_e\bar{p}$, i.e.,

$$\bar{A}_i = A_e \bar{p} \quad , \tag{13}$$

Equation (11) becomes

$$\dot{\tilde{p}} + \eta A_e \tilde{p} = \eta \tilde{A}_i \quad . \tag{14}$$

A sinusoidal pressure response requires that

$$\tilde{p} = \tilde{p}_{amp} \sin \omega t \quad , \tag{15}$$

where $\tilde{p}_{amp}$ is the amplitude. Combining Equations (14) and (15) yields

$$\tilde{A}_i = A_e \tilde{p}_{amp} \sin \omega t + \frac{\omega}{\eta} \tilde{p}_{amp} \cos \omega t \tag{16}$$

$$= \tilde{p}_{amp} \left(A_e^2 + \frac{\omega^2}{\eta^2}\right)^{\frac{1}{2}} \sin\left[\omega t + \tan^{-1}\left(\frac{\omega}{\eta A_e}\right)\right] \quad .$$

Thus, the variable inlet area consists of a sinusoidal opening similar to the outlet opening used in the present SPG with maximum size

$$\tilde{A}_{i(max)} = \tilde{p}_{amp} \left(A_e^2 + \frac{\omega^2}{\eta^2}\right)^{\frac{1}{2}} \quad . \tag{17}$$

For very high frequency, Equation (17) gives

$$\tilde{p}_{amp} = \eta \tilde{A}_{i(max)}/\omega \quad ,$$

which is similar to Equation (9).

It is seen that a simple harmonic response given in Equation (15) is obtainable in an ideal inlet-modulated SPG if two inlet openings are used: the first one determines the average pressure according to Equation (13), and the second one determines the amplitude according to Equation (17). Since the amplitude and the average of the pressure are being modulated independently by separate openings, no restrictions are imposed on their range of variation except the two conditions set forth in the beginning of this discussion for all SPG's and the possible impractical opening size under certain operation conditions. The perfect sinusoidal pressure variation makes this inlet-modulation technique attractive for high-frequency, large amplitude applications.

Limitations on Performance

The two design conditions mentioned previously concerning frequency and flow can now be examined.

The natural frequency of the cylindrical cavity, f_c, is given by

$$f_c = \frac{C}{2}\left[\left(\frac{n}{L}\right)^2 + \left(\frac{\lambda_{ij}}{a}\right)^2\right]^{\frac{1}{2}} \quad , \tag{18}$$

where L is the cavity length, n = 0, 1, 2, ... is the longitudinal wave number, i and j are the tangential and radial wave numbers, respectively. The first few λ_{ij} are

$$\begin{aligned} \lambda_{01} &= 1.2197 \\ \lambda_{02} &= 2.2331 \\ \lambda_{10} &= 0.5861 \\ \lambda_{20} &= 0.9722 \\ \lambda_{30} &= 1.3373 \quad . \end{aligned} \tag{19}$$

For a thin cavity, the lowest resonance frequency occurs at n = 0, i = 1,

$$f_{c(min)} = \frac{C}{2}\,\frac{\lambda_{10}}{a} = 0.293\,\frac{C}{a} \quad .$$

For the existing OM-SPG, a = 0.375 inch, f_c = 11,560 cps for nitrogen (C = 1151 ft/sec), and f_c = 33,370 for helium (C = 3321 ft/sec). Severe harmonic distortion usually appears at flow-modulation frequencies about half of these values. From Equation (10), it is seen that this is due to the resonance condition at the second harmonic. Inlet-modulation should improve this distortion because according to Eauation (15) there is no higher harmonic excitation present in the system.

The critical flow will be maintained for most gases if

$$\tilde{p}_{amp} + \bar{p} < 0.5 \quad .$$

For exit modulation, use of Equations (7) and (8) gives

$$2\,\frac{A_i}{A_{em}} + \frac{\eta\, A_i}{\omega} < 0.5 \quad . \tag{20}$$

For inlet modulation, use of Equations (13) and (17) gives

$$\frac{\tilde{A}_{i(max)}}{\left(A_e^2 + \frac{\omega^2}{\eta^2}\right)^{\frac{1}{2}}} + \frac{\bar{A}_i}{A_e} < 0.5$$

or

$$\frac{\eta\, \tilde{A}_{i(max)}}{\omega} + \frac{A_i}{A_e} < 0.5 \text{ for high frequencies.} \qquad (21)$$

Comparing Equations (20) and (21) shows that if opening sizes similar to that in the existing SPG are used in the inlet-modulated generator, similar amplitude can be obtained. However, $\tilde{A}_{i(max)}$ can be increased to increase the amplitude without affecting the essential sinusoidal pressure variation. Note that the factor 2 in Equation (20) limits $A_i/A_{em} < 1/4$ [actually used $A_i/A_{em} = (0.055/0.125)^2 = 0.194$] while larger ratios are permissible in Equation (21) so that increase of $\tilde{A}_{i(max)}$ is practical. For example, the present SPG, when using helium, gives

$$2\frac{A_i}{A_{em}} + \frac{\eta\, A_i}{\omega} = 0.388 + \frac{0.085}{f} \begin{cases} = 0.473 \ (f = 1 \text{ kc}) \\ = 0.397 \ (f = 10 \text{ kc}) \end{cases}$$

If the same inlet and outlet opening sizes are used as the constant openings for a given inlet-modulated cavity with helium and the inequality of (21) is written for 10 kc as an equality,

$$\frac{\eta\, \tilde{A}_{i(max)}}{\omega} + \frac{A_i}{A_e} = 0.397$$

or

$$\tilde{A}_{i(max)} = (0.397 - 0.194) \times 0.28 = 0.0569 \text{ in.}^2 ,$$

giving a diameter of 0.27 inch, which is greater than the present 0.055 inch and a peak-to-peak amplitude of 40 percent.

Discussion

From the above description of the current state of transducer-calibration techniques, it is concluded that the acoustic resonators can produce sinusoidal pressure waves only at frequencies less than a few hundred cycles per second.

The fixed-mass, variable-volume system seems to offer a neat, simple apparatus at wide frequency spectrum. However, many technical areas have to be explored before this wide spectrum can be fully utilized to advantage. For example, the double-crystal system does not have the problem of fluid leakage. However, the constraint at the crystal edge will severely limit the motion of the crystals, which in turn restricts the pressure amplitude obtainable. On the other hand, seal O-rings can be used on the piston. However, this will greatly increase the reactance of the system which again reduces drastically the pressure amplitude. Thus, current generators of this type are either for low-frequency calibration ($\sim$ 2,000 cps) or for low amplitude (<1 percent of static pressure) at high frequencies ($\sim$ 10,000 cps). The inadequacy of theoretical analysis and the lack of an energetic driver leaves the field of high-amplitude and high-frequency fixed-mass cavity completely unexplored. Regardless of the driver used, the diametrical dimension will limit the operable high frequencies because of the presence of higher harmonics in the fluid even under a simple harmonic driver. This can be seen from the equation developed previously,

$$\frac{P_o - P}{P_o} = 1 - (1 + \alpha \sin \omega t)^{-\gamma} = \alpha \gamma \sin \omega t - \frac{\alpha^2}{2} \gamma (\gamma + 1) \sin^2 \omega t + \ldots$$

For large amplitude, the clearance has to be small ($<$0.1 inch) and precise when assembled.

The variable-mass, fixed-volume system is capable of producing large amplitudes ($\sim$ 5 percent of the biased pressure) at high frequencies ($\sim$ 10,000 cps) with little harmonic distortion. At lower frequencies, the amplitudes will become increasingly large (Figure 8). Though the existing OM-SPG is structurally capable of being operated at a maximum biased pressure of 1000 psi, all work so far has been carried out at a pressure of around 250 psi. As far as performance is concerned, this system seems to be the most promising among all that can achieve a dynamic pressere at large amplitude over a wide frequency and average pressure spectrum.

In both the fixed-mass and variable-mass systems, attractive potentials as transducer-calibration devices exist which are technologically challenging and need to be explored in the future.

For the fixed-mass system, though the dynamic pressure may degenerate into sawtooth form at high frequency and high amplitude, any prediction at present is purely conjectural. The immediate area of exploration seems to be the development of an energetic high-frequency, large-displacement driver.

Development of a double cavity crystal driven SPG is currently under contract with the USAF Rocket Propulsion Laboratory at Edwards Air Force Base, Edwards, California.

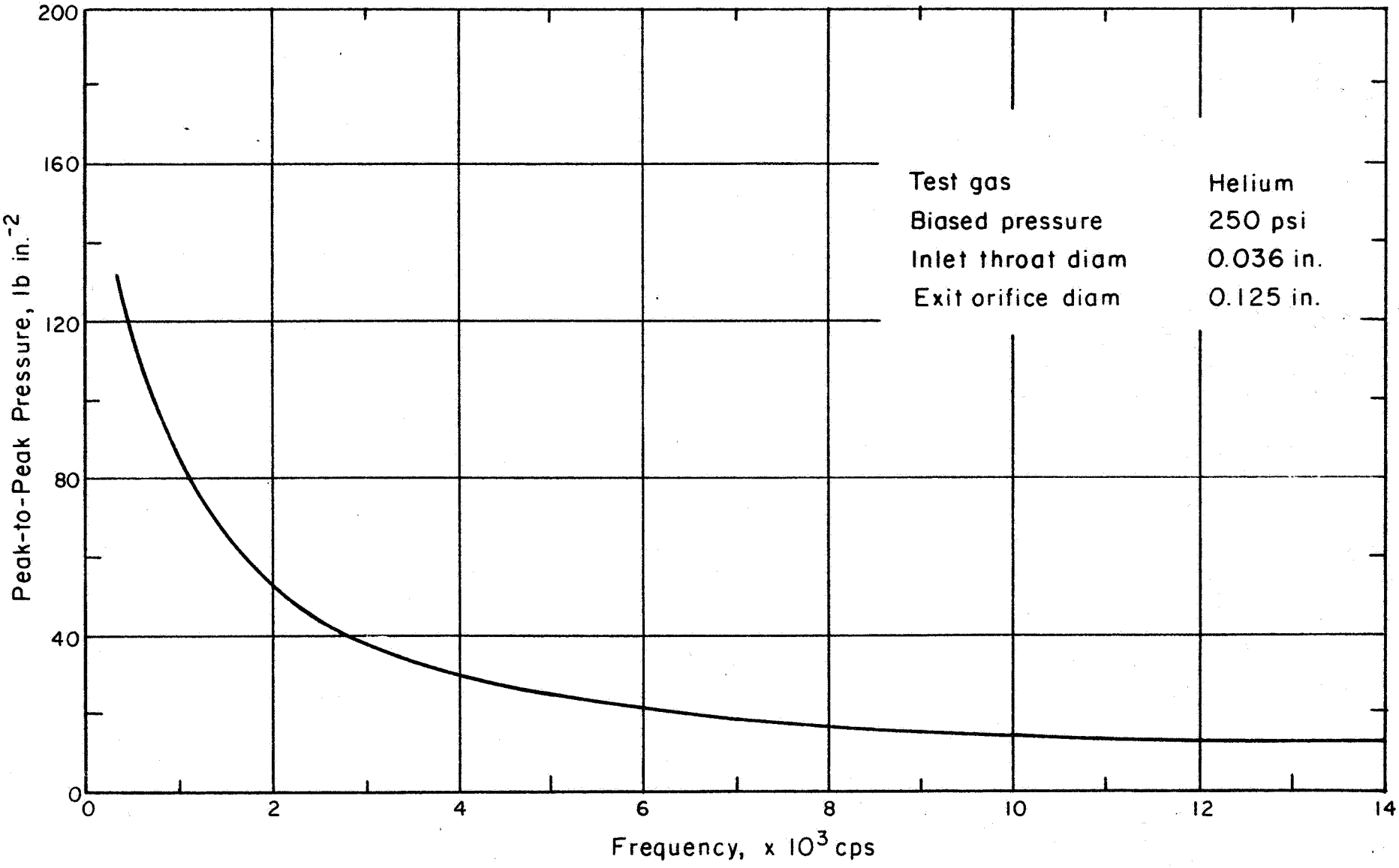

FIGURE 8. PEAK-TO-PEAK PRESSURES VS FREQUENCY FOR PRINCETON SINUSOIDAL PRESSURE GENERATOR. (Reference 6)

For the variable-mass system, it is seen that the amplitude can be increased if inlet- instead of outlet-flow modulation is used. Because of the absence of higher harmonic excitation in inlet-flow modulation, it would appear that the operation frequency can be increased closer to the first resonance frequency ($\sim$ 33,000 cps with helium). Further increase of the frequency is possible by utilizing very high temperature gas. However, this may require complicated cooling systems for the cavity. Except for specialized transducers, exposure directly to the hot gas can cause damage. It should be noted that any of the existing outlet-modulated units can be easily converted into an inlet-modulated one for preliminary test evaluation, since all the accessories for operation, such as instrumentation, power, and gas supply systems, would be the same for both kinds of generators.

INLET-MODULATED SPG EVALUATION

Based on the findings of the exploratory analytical study of the various methods of generating large amplitude, high-frequency sinusoidal pressure oscillations at high static pressures, the technical direction of the program was changed to explore the inlet-modulated SPG rather than the resonant free-piston oscillator. The analyses had indicated the possibility of using the present NASA OM-SPG to perform inlet-modulated tests. Therefore, an investigation was made to determine the possibility and extent of the use of the OM-SPG to explore the IM-SPG concept. It was also desired that no modification be made that would affect its performance or prohibit its continuing use as an outlet-modulated SPG at the completion of the present contract.

The investigation studied the IM-SPG concept to determine its mechanical design requirements. These requirements were then compared with the OM-SPG mechanical design to determine how much of the IM-SPG concept could be tested without permanent modification to the OM-SPG. An analysis was then made to determine the theoretical IM-SPG performance of the test device.

Design Comparisons

The outlet-modulated SPG design concept is shown in Figure 9.

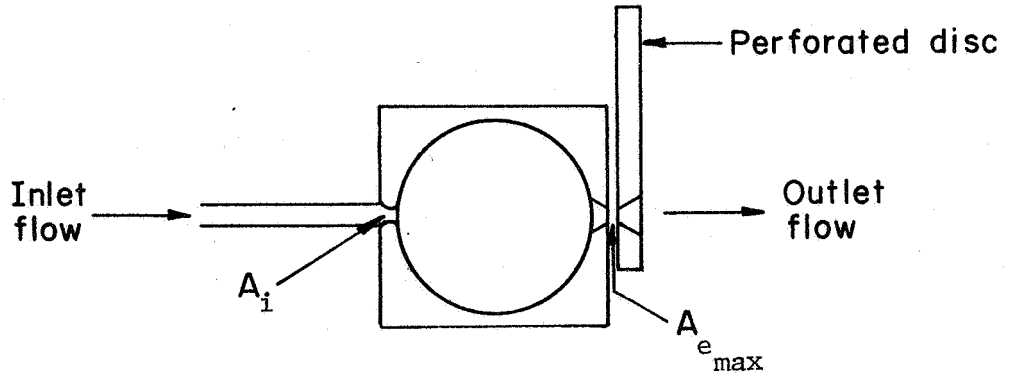

FIGURE 9. OUTLET-MODULATED SINUSOIDAL PRESSURE GENERATOR

It is seen to consist of a cylindrical chamber, with two diametrically opposed holes. Gas enters the chamber through one hole and exits through the other. It is a variable-mass, fixed-volume generator or a flow-through device. The flow through the outlet area is modulated by a rotating disc which contains holes in a circular pattern spaced with a diameters distance between them.

The inlet-modulated design concept, Figure 10, is also a variable-mass, fixed-volume generator. Thus, at least two holes are also required,

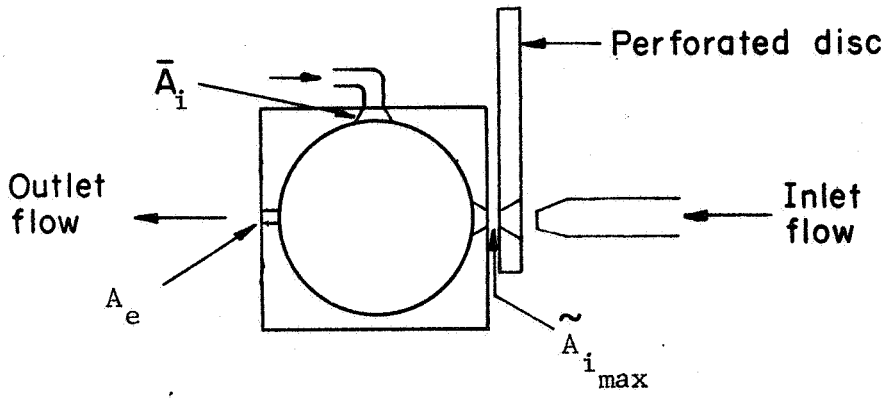

FIGURE 10. INLET-MODULATED SINUSOIDAL PRESSURE GENERATOR

a gas inlet hole and a gas outlet hole. In the inlet-modulated concept, there is no outlet area modulation and it need be only a constant area. The most general or versatile design has two inlet areas and was described in the previous section. In this design, one area is constant and the other variable. These two separate inlet areas allow the mean pressure to be controlled independently of the dynamic pressure. Equation (17) shows that the variable area is a function of both the dynamic pressure amplitude and the frequency. Thus, for a specific $\tilde{A}_i$, the dynamic pressure amplitude would vary inversely with frequency.

Separate control of the frequency effects on dynamic pressure could be obtained by making the required variable inlet area into two separate variable or modulated inlets, having respective maximum openings $\tilde{A}_{i1}$ and $\tilde{A}_{i2}$ according to

$$\tilde{A}_{i1} = A_e \tilde{p}_{amp} \tag{22}$$

$$\tilde{A}_{i2} = \frac{\omega}{\eta} p_{amp} = \left(\frac{\omega}{\eta}\right) A_{i1}/A_e \quad . \tag{23}$$

Two variable areas and, therefore, two rotating discs are required.

From the above, it is seen that to test all of the inlet-modulated SPG concept and to evaluate its potential performance would require one outlet hole and a minimum of two inlet holes, one constant and one to be modulated. Thus, at least three holes are required. The present OM-SPG has two holes, A third hole, which would allow average pressure variation, could be added.

The test with the least modification to the present device would be the single inlet, single outlet case. With only one inlet area, there is a single valued relationship between dynamic pressure amplitude, mean or average pressure, and frequency. Thus, there would not be separate control of the average and dynamic pressures. The present OM-SPG also has a similar single valued relationship (see Figure 8). The major difference between the two is that the inlet-modulation does not produce a higher harmonic frequency dependent term in the pressure variation like that of outlet modulation, i.e. $(\eta A_e/2\omega)(\cos \omega t + \frac{1}{4} \cos 2 \omega t)$. Such a higher harmonic term causes harmonic distortion (deviation from pure sinusoidal variation) and could excite resonance at a low frequency, thereby limiting the usable frequency range. In addition, inlet-modulation allows larger dynamic pressures at each average pressure, by nearly a factor of two for any specified maximum allowable hole in the SPG. This factor was mentioned in the previous section.

To use the present OM-SPG to investigate the IM-SPG concept requires that the present outlet hole size and associated wheel, and inlet hole be compatible. It also remains to determine the resulting dynamic pressures, average pressures, and frequencies that can be obtained with a hole the size of, or smaller than, the present OM-SPG entrance hole.

Single Inlet Analysis

We will now determine the required flow areas and pressures for the IM-SPG using a single inlet. From Equation (11), the pressure expression in terms of inlet and outlet areas is

$$\dot{\tilde{p}} + \eta A_e \tilde{p} = \eta(A_i - A_e \bar{p}) \qquad (11)$$

$$= \eta\left[\frac{A_{im}}{2} (1 + \cos \omega t)\ 2 A_e \bar{p}\right]$$

$$\dot{\tilde{p}} + \eta A_e \tilde{p} = \eta\left[\frac{A_{im}}{2} (1 + \sin(\omega t + \tfrac{\pi}{2})) - A_e \bar{p}\right] \quad , \qquad (24)$$

where A_{im} is the maximum inlet area (A_i is the average inlet area).

A sinusoidal pressure variation requires that

$$\tilde{p} = \tilde{p}_{amp} \sin(\omega t - \phi) \quad , \qquad (25)$$

and, therefore,

$$\dot{\tilde{p}} = \omega\, \tilde{p}_{amp} \cos(\omega t - \phi) = \omega\, \tilde{p}_{amp} \sin(\omega t - \phi + \tfrac{\pi}{2}) \quad . \qquad (26)$$

Substitution of (25) and (26) into (24) gives

$$- \omega \tilde{p}_{amp} \cos (\omega t - \phi + \frac{\pi}{2}) - \eta A_e \tilde{p}_{amp} \sin (\omega t - \phi) + \eta \frac{A_{im}}{2} - \eta A_e \bar{p} + \eta \frac{A_{im}}{2} \sin (\omega t + \frac{\pi}{2}) = 0 \quad . \tag{27}$$

It is seen that the sum of the third and fourth terms of Equations (27) must equal zero, i.e.,

$$\eta \frac{A_{im}}{2} - \eta A_e \bar{p} = 0 \quad , \tag{28}$$

which give the relationship between the inlet area, A_{im}, and the outlet area, A_e, for a specific average pressure, $\bar{p}$. Thus,

$$\bar{p} = \frac{A_{im}}{2 A_e} = \frac{1}{2} \left(\frac{d_{im}}{d_e}\right)^2 \quad . \tag{29}$$

The solution for the transient pressure, $\tilde{p}$, is

$$\tilde{p} = \frac{\eta A_{im}}{2 \sqrt{\omega^2 + \eta^2 A_e^2}} \sin \left[\omega t - \tan^{-1} \left(\frac{\eta A_e}{\omega}\right) \right] \quad . \tag{30}$$

The expression for the total dimensionless pressure, p^*, results from the combination of equations (29) and (30)

$$p = \bar{p} + \tilde{p} = \frac{A_{im}}{2A_e} + \frac{\eta A_{im}}{2 \sqrt{\omega^2 + \eta^2 A_e^2}} \sin \left[\omega t - \tan^{-1} \left(\frac{\eta A_e}{\omega}\right) \right] \quad . \tag{31}$$

The relationship between pressure amplitude and the flow area is, from Equation (31),

$$p^* = \frac{A_{im}}{2A_e} \left[1 + \frac{\frac{\eta A_e}{\omega}}{\left[1 + \left(\frac{\eta A_e}{\omega}\right)^2\right]^{\frac{1}{2}}} \right] \quad . \tag{32}$$

Noting that Equations (29) and (30) give

$$\frac{\tilde{p}}{\bar{p}} = \frac{\dfrac{\dfrac{\eta A_{im}}{\omega}}{2\sqrt{1 + \left(\dfrac{\eta A_e}{\omega}\right)^2}}}{\dfrac{A_{im}}{2 A_e}} = \frac{\dfrac{\eta A_e}{\omega}}{\left[1 + \left(\dfrac{\eta A_e}{\omega}\right)^2\right]^{\frac{1}{2}}} \quad . \tag{33}$$

From Equation (5) and Equation (29) or by substitution of Equation (33) into Equation (32) the p^* is found as

$$p^* = \frac{A_{im}}{2 A_e}\left[1 + \frac{\tilde{p}}{\bar{p}}\right] \quad . \tag{34}$$

From the above expressions, the various area, or hole, requirements can be determined for various pressure conditions. One of the fundamental requirements of the modulated SPG's is critical flow. Critical flow conditions require that $\bar{p} < 1/2$ for steady flow and that $\bar{p} + \tilde{p} < 1/2$ for varying flow. This in turn requires, as may be seen from Equation (29), $d_{im} < d_e$. In the present SPG, the outlet diameter is 0.125 inch and the inlet diameter is 0.055 inch. Thus, reversing the flow direction to obtain inlet modulation would give $d_{im} = 0.125$ inch and $d_e = 0.055$ inch and, therefore, $d_{im} > d_e$. The value of d_e can conveniently be increased up to 0.2 inch simply by changing nozzle inserts. Anything larger than that will require only machining a larger nozzle insert hole (or making a new SPG chamber to prevent modification to the present SPG).

Considering $d_e = 0.2$, the exit area is

$$A_e = 0.7854\ (0.2)^2 = 0.0314\ \text{inch}^2$$

and

$$\bar{p} = \frac{1}{2}\left(\frac{0.125}{0.2}\right) = 0.195 < 0.5 \quad .$$

The predicted ratio of peak-to-peak pressure to average chamber pressure, expressed in percentages for nitrogen and helium as a function of frequency is

$$\frac{\text{P-t-P}}{P_c} = \frac{2\tilde{p}}{\bar{p}} = \begin{cases} N_2; \\ He; \end{cases}$$

	1 kc	2 kc	4 kc	6 kc	8 kc	10 kc
N_2;	70.8	37.8	19.1	12.8	9.6	7.6
He;	144.8	93.8	45.0	34.5	23.1	21.0

For comparison, the theoretical performance of the present SPG is

$\frac{2\tilde{p}}{\bar{p}}$ =		1 kc	2 kc	4 kc	6 kc	8 kc	10 kc
	N_2;	14.96	7.48	3.74	2.5	1.86	1.5
	He;	42.0	21.0	10.5	7.0	5.24	4.2

The performance (peak-to-peak dynamic pressure) of the present outlet modulated with a maximum hole size corresponding to that being used in the inlet-modulation test (d = 0.2 inch) is approximately one half that of the inlet-modulated design. This may be seen by comparing the expression for $\frac{\tilde{p}}{\bar{p}}$ of the outlet-modulated SPG with Equation (34)

$$\frac{\tilde{p}}{\bar{p}} = \frac{\eta A_e}{\omega} \quad . \tag{35}$$

Critical flow is maintained as seen from Equation (34) and the values for $\frac{\tilde{p}}{\bar{p}}$, i.e.,

$$p = \bar{p} + \tilde{p} = 0.195 \left(1 + \frac{\tilde{p}}{\bar{p}}\right) < 0.4 \quad .$$

OUTLET-MODULATED SPG TESTING

A series of outlet-modulated SPG performance tests were made to provide data at the same pressure and frequency conditions contemplated for the inlet-modulated SPG tests. These data were to serve as a reference to determine performance improvements of the inlet-modulated concept and to provide design information for the new concept. One of the two proposed major advantages of the inlet-modulated concept is the elimination of higher harmonic components predicted in the pressure wave of the outlet-modulated design. If the magnitude of the higher harmonic components are greater than other noise existing in the pressure signal, their elimination should increase the usable frequency range of the choked flow, siren-type device. Such an increase offers two advantages: first it permits calibrations at higher frequencies, and second, it extends the usable frequency ranges of lower cost gases such as nitrogen or air. The other proposed performance advantage for the inlet-modulated concept is an increased dynamic to static pressure ratio. This also will reduce gas requirements and costs.

Before any tests were made, the present SPG was inspected to ensure that the unit was in proper operating order. This checkout included checking of parts alignment, clearance setting, bearing runout, etc. The clearance between the perforated disc and the chamber block was found to

vary by 0.0035 inch during a full rotation of the disc. This variation is of the same order as the clearance which is normally between 0.002 and 0.005 inch. Further inspection showed that this variation was caused by two factors: the disc flatness varying several thousands of an inch, and the shaft on which the disc is mounted was misaligned, or out of perpendicularity with the disc. The shaft alignment was improved and two thousandths of an inch was machined off of the disc, correcting disc flatness to approximately one ten thousandth of an inch. The resulting maximum clearance variation during a revolution was less than one-half of a thousandth of an inch.

Both the average pressure and dynamic pressure envelopes were found to vary over a complete wheel revolution. The variations are attributed to variation of the clearance between the perforated disc and block and was minimized by the previously mentioned machining. Static tests with the disc closing the chamber outlet and with the outlet opened, showed the disc deflecting approximately 0.001 inch with a 100 psia chamber pressure. Since no new (higher strength) disc was planned for this program, this variation was tolerated and accounted for in the inlet-modulation tests. In these latter tests, the pressure loading is in the direction that tends to deflect the disc into the chamber body. Proper clearances to allow for this movement were provided.

Approximately 150 tests were made including the checkout tests. Nitrogen and helium were used as the test gases with nitrogen being used for the majority of the tests. Three different average chamber pressure ranges were investigated--50, 100, and 250 psia. For each of these average chamber pressures, three different spacings between the rotating disc and chamber body were studied--0.001, 0.003, and 0.005 inch. For each of the nine pressure-spacing combinations, the frequency was varied. The majority of the frequency variation tests were at the 100-psia level. For those 100-psia tests, the frequency was varied from 200 cps to 10,000 cps. The matrix of test conditions is shown in Table 1. From this test sequence, the SPG performance at various pressure levels for various disc-chamber body spacing and for different test gases were estimated over the normal frequency range of the SPG.

The primary test data were the dynamic chamber pressures which were measured with a high resonant frequency dynamic pressure transducer and were recorded by photographing their oscilloscope traces. In addition, the SPG entrance pressure was measured with a pressure gage on each test, and the average chamber pressure was measured with a pressure gage over a series of test conditions. Electrical power used by the disc drive motor was also measured over a series of test conditions.

The dynamic pressure performance data is shown in Figure 11 by the curves labeled (1) and (3). Curve (1) is for the nitorgen tests and Curve (3) is for the helium tests. Only two curves for outlet-modulation are shown. Within the accuracy of the data (oscillograph pictures) the dynamic pressure amplitude and wave shape were both found to be essentially independent of the bias or average chamber pressure conditions tested. Comparison of these curves with the predicted performance given on Pages 42 and 43 shows excellent agreement. The nitrogen results are shown only to 4000 hertz above which the wave shape became unacceptable.

TABLE 1. OUTLET-MODULATED TEST MATRIX

Frequency, cps	Chamber Pressure, psia: 50						100						250					
	Clearance, inches: 0.001		0.003		0.005		0.001		0.003		0.005		0.001		0.003		0.005	
	Gas: N_2	He	N_2	He	N_2	He	N_2	He	N_2	He	N_2	He	N_2	He	N_2	He	N_2	He
200			x	x	x	x	x		x	x	x	x			x	x	x	
400									x		x			x		x		x
600			x	x	x	x			x	x	x	x			x	x	x	x
800									x		x							
1,000			x	x	x	x	x		x	x	x	x		x	x	x	x	x
1,250									x		x							
1,500									x		x							
2,000									x		x							
2,500									x		x							
3,000							x		x		x							
4,000									x		x							
5,000			x	x	x	x	x		x		x	x		x	x	x	x	x
6,000									x		x							
8,000									x		x							
9,000									x									
10,000			x	x	x	x			x	x	x	x		x	x	x	x	x
11,000									x									
11,500									x									
12,000									x									
12,500									x									
13,000									x									
13,500									x									
14,000									x									

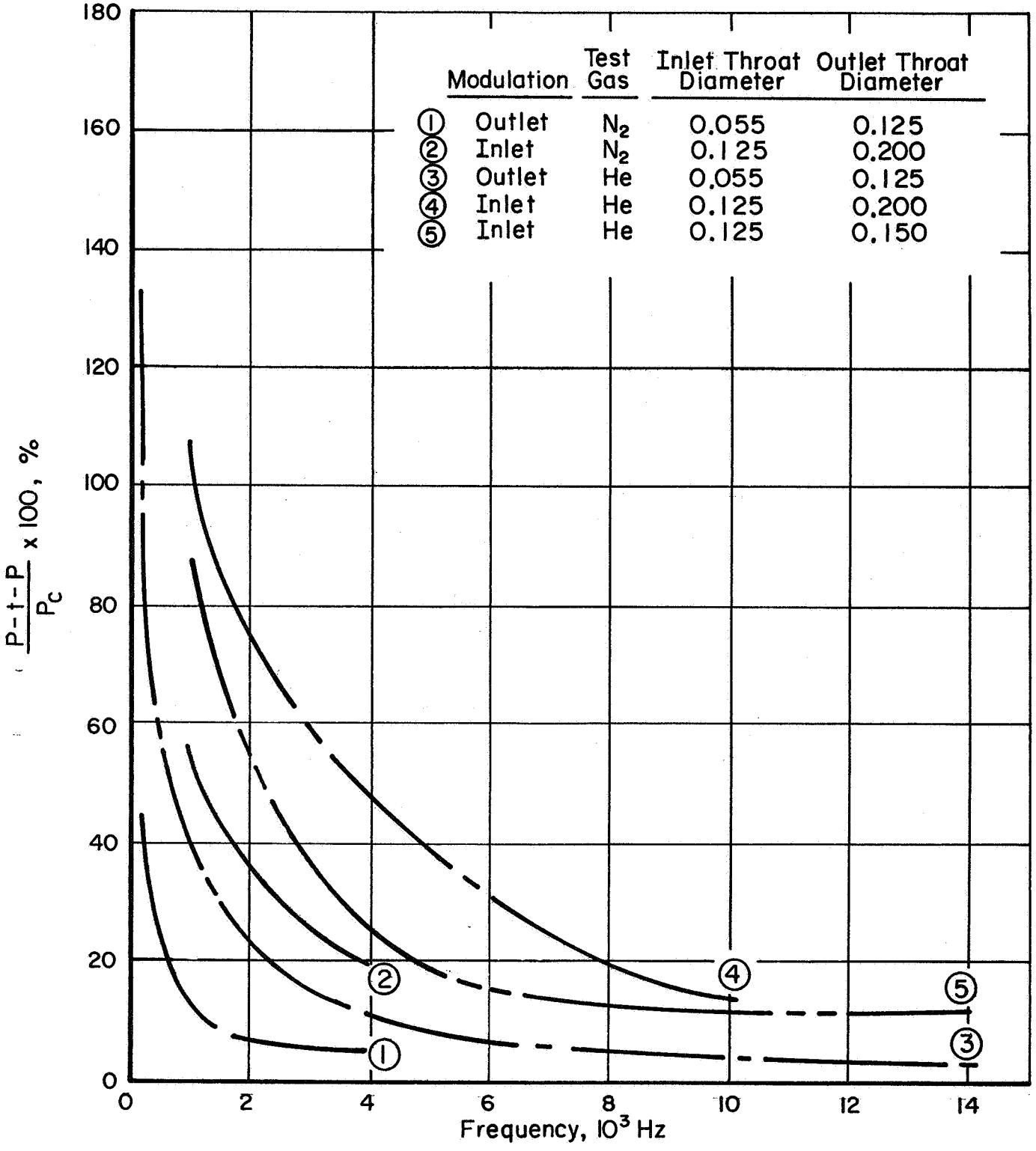

FIGURE 11. PERCENT PEAK-TO-PEAK PRESSURE TO CHAMBER PRESSURE VERSUS FREQUENCY FOR OUTLET AND INLET MODULATED SINUSOIDAL PRESSURE GENERATORS

INLET-MODULATED SPG TESTING

The inlet-modulated concept was tested using the present NASA outlet-modulated SPG. In principle, this was done by reversing the flow direction through the present OM-SPG. To accomplish reverse flow-through requires a flow entrance component mounted next to the rotating disc and an adjustable mounting system for it which will allow accurate alignment and spacing. A new nozzle and retainer is also required for the exit (entrance nozzle in outlet-modulated form) in order to maintain critical flow.

The nozzle, its retainer, and the flow inlet adaptor were designed, fabricated, and assembled to form the inlet-modulated test device. This test device is pictured in Figure 12.

The test plan selected was to test initially at some of the test conditions used in the outlet-modulated testing program. The program was then to be modified in accordance with test results as appropriate. The resulting matrix of tests is shown in Table 2. In all, over 50 inlet-modulated tests were made.

The general dynamic pressure amplitude results are shown in Figure 11 as curves (2), (4), and (5). For these tests only one disc-body clearance was used, 0.0025 inch. The clearance between the disc and the flow inlet adaptor was 0.0015 inch. The outlet throat diameter was later reduced from 0.200 inch to 0.150 because the flow system was flow limited at the high flow rate-high pressure helium tests.

The amplitudes of the inlet-modulated tests are seen to be much larger than those of the outlet-modulated tests for all conditions investigated. The amplitudes of tests with the 0.200 inch outlet throat diameter is seen from Pages 42 and 43 to compare very well in the middle and high frequency ranges with the theoretical predictions. The tests results are below those predicted in the lower frequency range. The larger dynamic pressure amplitude of the inlet-modulated tests are due to the use of a larger inlet to outlet flow area ratio and larger flow areas. As previously discussed the use of a larger area ratio is one of the advantages of the inlet-modulated concept. The predicted amplitude of the IM-SPG test device should be approximately 4 times that of the present OM-SPG based on the ratio of area ratios and the ratio of maximum areas. These was essentially the results obtained as seen in Figure 11. Also, if the OM-SPG 0.125 inch diameter outlet hole is scaled to 0.2 inch and the same area ratio is used, the inlet-modulated is predicted to be 3.5. Thus, the inlet-modulated concept offers a 40 percent larger dynamic pressure than can be obtained with equal maximum flow hole sizes in the OM-SPG.

Generally, the IM-SPG wave shape was always at least as good as the OM-SPG and somewhat better at the higher frequencies for helium. The wave shape performance was essentially the same for both units using nitrogen. Both wave shapes degenerated rather badly around 4000 hertz and not in a manner that could be directly associated with the harmonic conditions predicted. Some of the wave shape characteristics obtained with helium are shown in Figure 13.

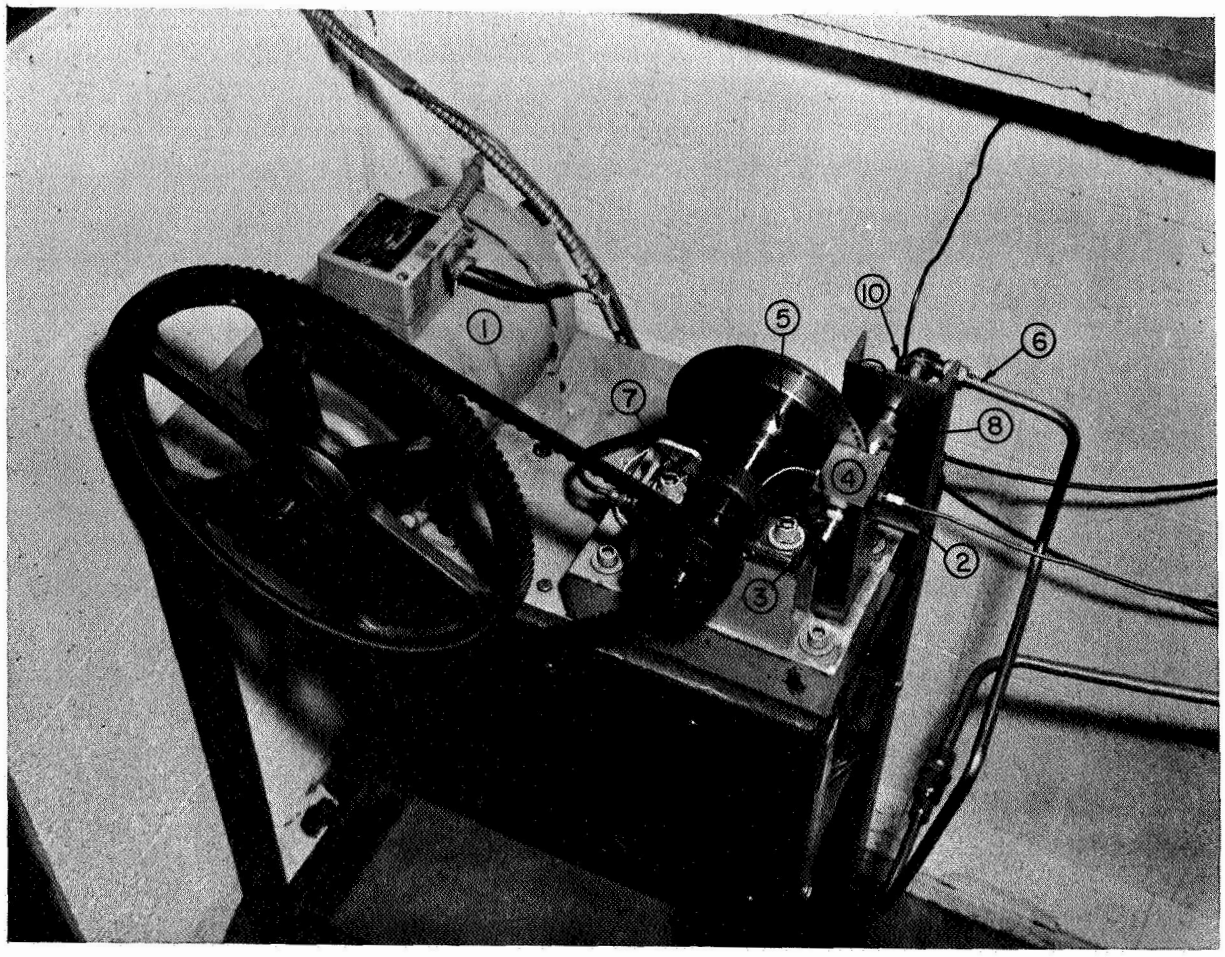

FIGURE 12

INLET-MODULATED SINUSOIDAL PRESSURE GENERATOR

1. Variable-speed drive motor
2. Average chamber pressure gage line
3. Reference dynamic pressure transducer
4. Pressure chamber
5. Rotating disk with multiple flow ports
6. Inlet gas supply line
7. Revolution counter and instrument triggering pickup
8. Inlet flow nozzle
9. Nozzle mount
10. Inlet pressure gage line

TABLE 2. INLET-MODULATED SPG TEST MATRIC

Frequency, cps	Gas	
	N_2	He
1,000	x	x
1,250	x	
1,500	x	
2,000	x	x
2,500	x	
3,000	x	
4,000	x	
5,000	x	x
6,000	x	x
7,000		
8,000	x	x
9,000		x
10,000	x	x
11,000	x	x
12,000	x	
12,500		x
13,000	x	
13,500		x
14,000	x	x
15,000		

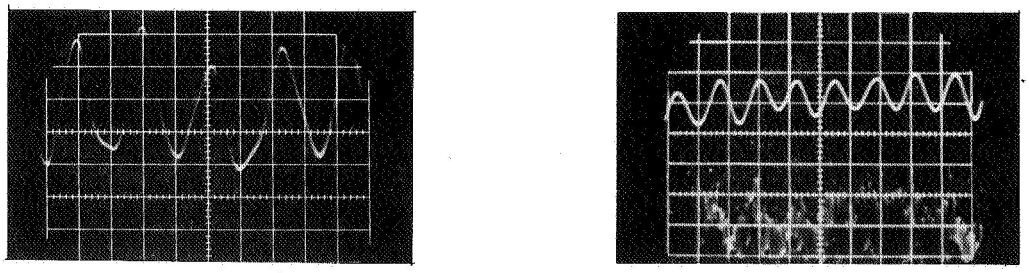

5,000 cps
Filter Cut-Off 10,000 cps

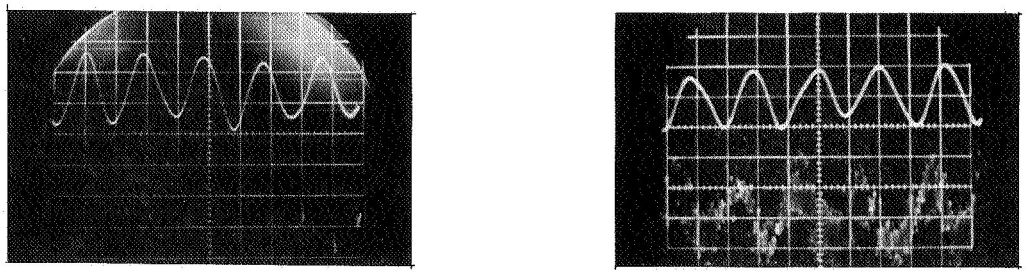

8,000 cps
Filter Cut-Off 20,000 cps

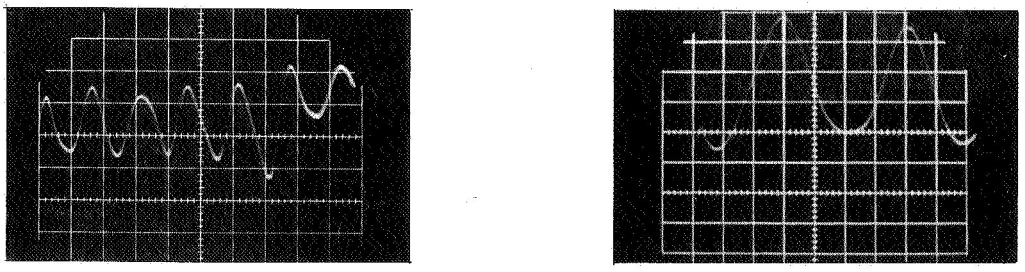

12,500 cps
Filter Cut-Off 20,000 cps

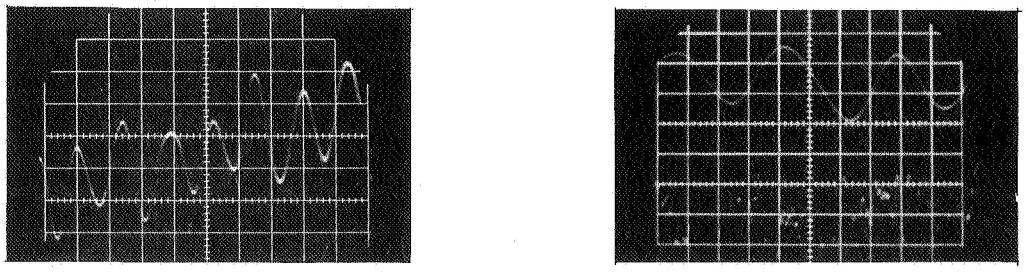

14,000 cps
Filter Cut-Off 20,000 cps

Inlet-Modulated Outlet-Modulated

FIGURE 13. CHAMBER RESPONSE WITH HELIUM

As can be seen from the photographs, the inlet and outlet modulated wave forms are similar at 5000 and at 8000 hertz. The OM-SPG waveform was somewhat more degenerative at 12,500 and 14,000 hertz than the IM-SPG. The degeneration again does not appear to be caused by the harmonic conditions predicted. The cyclic variation is attributed to disc deflections caused by the gas pressure loads. The tests would have been conducted at higher frequencies but this was prevented by excessive SPG vibrations. The vibrations can be eliminated with a higher strength disc and mounting systems, higher precision bearings, and dynamically balanced rotating parts. Because of the vibrations and possibly due to spurrious high frequency gas pressure components, the available pressure transducer required filtering on its output. The companion filter for the OM-SPG had lower cutoff frequencies of 10,000 and 20,000 cycles per second. Thus, the filters would have eliminated the higher harmonics predicted for the OM-SPG if they existed.

CONCLUSION AND RECOMMENDATIONS

From the analytical and experimental results obtained and presented in this report, it is concluded the inlet-modulated sinusoidal pressure generator is feasible, applicable, and has attainable performance suitable for transducer evaluations at large-amplitudes, high frequencies, and high-average pressures.

The analytical studies concluded that the IM-SPG concept offered the most promise of those concepts evaluated. A design was evolved which allowed testing of the major aspects of the concept by modification of the available sinusoidal pressure generator. The analyses also predicted that for the available chamber, which tended to fix limits on inlet and outlet flow passage sizes, larger dynamic pressure amplitudes can be obtained by inlet-modulation than by outlet modulation.

The inlet-modulation and outlet-modulation tests investigated the two basic premises of the concept; higher dynamic pressures for a given diameter chamber, and improved wave shapes at high frequencies. These investigations demonstrated that larger dynamic pressure amplitudes and higher usable frequencies could be obtained with an inlet-modulated sinusoidal pressure generator and are applicable for dynamic pressure transducer calibration. This new calibration capability is not, however, available for use. The investigations evaluated the IM-SPG concept. Analytical studies predicted the performance and experimental studies confirmed it. The experimental studies were conducted on a temporarily modified outlet-modulated sinusoidal pressure generator--no new IM-SPG has been built. In order to utilize the new calibration technology, an actual IM-SPG must be designed, developed and fabricated.

The modified OM-SPG is not suitable as an IM-SPG for calibration work because in its modified form it can operate only in a limited portion of the pressure-frequency range required. Also, it does not possess the strength for the desired higher pressure conditions, the inlet and outlet flow passages are not properly sized and shaped, and the necessary alignment and adjustment mechanisms are not provided.

It is recommended that an inlet-modulated sinusoidal pressure generator capable of operating at static or average chamber pressures of 1500-2000 psia be built. In addition, it is recommended that the unit be designed for both hydrogen and vacuum operation.

Hydrogen offers higher frequency and better waveshape and capability because of its higher speed of wave propagation or speed of sound. To accommodate hydrogen operation, the IM-SPG should probably be encased in a gas tight housing and the entire system including the gas storage reservoir, the connecting lines, the enclosed IM-SPG, and the exhaust ducting covered with a forced draft hood type system. The IM-SPG housing and exhaust ducting could also be used with a vacuum pump to extend the range of application of the calibrator. Pressure transducers used in wind tunnel, jet engine, and fluidic application could then be calibrated.

It is also recommended that all future SPG designs include accurate adjusting and alignment mechanisms. Further, the designs should be very "stiff", i.e., have minimum interference from structural vibrations, negligible bending, and deflection, since alignment proved to be difficult, time consuming, and a critical part of the present program.

Most of the presently used dynamic pressure transducers have had some sort of dynamic calibration. The calibrations have not been made on a consistent reference so that a real comparison and evaluation can be made. Also, none of the transducers have been calibrated at the advanced pressure conditions and improved waveshapes that the recommended IM-SPG should have. It is recommended that a series of calibrations be performed of the most frequently used current dynamic pressure transducers.

REFERENCES

(1) Betchov, R., "Non-linear Oscillation of a Gas Column", Phys. Fluids, 1, 205 (1958).

(2) Schmidt, E., "Large Amplitude Oscillation of Gas Columns in Piping (in German)", Z. VDI 79, No. 22 (1935).

(3) Schweppe, J. L., Eichberger, L. D., Muster, D. F., Michaels, E. L., and Paskusz, G. F., "Methods for the Dynamic Calibration of Pressure Transducers", National Bureau of Standards Monograph 67 (1963).

(4) Heidmann, M. F., "Strong, Traveling, Transverse Acoustic Modes Generated by a Rotating Gas Jet", AIAA Journal, Vol. 5, No. 11, (November, 1967).

(5) Morefield, R. I., "Dynamic Comparison Calibrator for High Range Pressure Transducers", Proceedings, Inst. Environmental Sc. (1965).

(6) Thomas, J. P., and Layton, J. P., "Final Summary Technical Report on Transient Pressure Measuring Methods Research", Princeton University AMS Report No. 595Z, (March 31, 1967).

DISTRIBUTION LIST

NASA Headquarters (1)
Washington, D. C. 20546
Attention: Contracting Officer, BCA

NASA Headquarters (1)
Washington, D. C. 20546
Attention: Patent Office, AGP

NASA Lewis Research Center (1)
21000 Brookpark Road
Cleveland, Ohio 44135
Attention: Office of Technical Information

NASA Lewis Research Center (1)
21000 Brookpark Road
Cleveland, Ohio 44135
Attention: Contracting Officer

NASA Lewis Research Center (1)
21000 Brookpark Road
Cleveland, Ohio 44135
Attention: Patent Office

NASA Marshall Space Flight Center (2)
Huntsville, Alabama 35812
Attention: Office of Technical Information, MS-IP

NASA Marshall Space Flight Center (1)
Huntsville, Alabama 35812
Attention: Technical Library

NASA Marshall Space Flight Center (1)
Huntsville, Alabama 35812
Attention: Purchasing Office, PR-EC

NASA Marshall Space Flight Center (1)
Huntsville, Alabama 35812
Attention: Patent Office, M-PAT

NASA Marshall Space Flight Center (1)
Huntsville, Alabama 35812
Attention: Keith Chandler, R-P&VE-PA

NASA Marshall Space Flight Center (1)
Huntsville, Alabama 35812
Attention: Technology Utilization Office, MS-T

NASA Pasedena Office (1)
4800 Oak Grove Drive
Pasadena, California 91103
Attention: Patents and Contracts Management

Western Support Office (1)
150 Pico Boulevard
Santa Monica, California 90406
Attention: Office of Technical Information

NASA Lewis Research Center (1)
21000 Brookpark Road
Cleveland, Ohio 44135
Attention: Marshall Burrows, Technical Director

NASA Headquarters (4)
Washington, D. C. 20546
Attention: Chief, Liquid Propulsion Technology,RPL

NASA Scientific and Technical Information
Facility (25)
P. O. Box 33
College Park, Maryland 20740

NASA Headquarters (1)
Washington, D. C. 20546
Attention: Mr. Vincent L. Johnson, Director
Launch Vehicles and Propulsion, SV
Office of Space Science and Applications

NASA Headquarters (1)
Washington, D. C. 20546
Attention: Mr. Edward Z. Gray, Director
Advanced Manned Missions, MT
Office of Manned Space Flight

NASA Ames Research Center (1)
Moffett Field, California 24035
Attention: Leonard Roberts
Mission Analysis Division

NASA FIELD CENTERS

Ames Research Center (2)
Moffett Field, California 94035
Attention: H. J. Allen
Mission Analysis Division

Goddard Space Flight Center (2)
Greenbelt, Maryland 20771
Attention: Merland L. Moseson, Code 620

Jet Propulsion Laboratory (2)
California Institute of Technology
4800 Oak Grove Drive
Pasadena, California 91103
Attention: Henry Burlage, Jr.
Propulsion Division, 38

Langley Research Center (2)
Langley Station
Hampton, Virginia
Attention: Dr. Floyd L. Thompson, Director

Lewis Research Center (2)
21000 Brookpark Road
Cleveland, Ohio 44135
Attention: Dr. Abe Silverstein, Director

Marshall Space Flight Center (2)
Huntsville, Alabama 35812
Attention: Hans G. Paul, Code R-P&VED

Manned Spacecraft Center (2)
Houston, Texas 77001
Attention: Dr. Robert R. Gilruth, Director

Western Operations Office
150 Pico Boulevard
Santa Monica, California 90406
Attention: Robert W. Kamm, Director

John F. Kennedy Space Center, NASA (2)
Cocoa Beach, Florida 32931
Attention: Dr. Kurt H. Debus

GOVERNMENT INSTALLATIONS

Aeronautical Systems Division (1)
Air Force Systems Command
Wright-Patterson Air Force Base
Dayton, Ohio 45433
Attention: D. L. Schmidt, Code ASRCNC-2

Commander (1)
Office of Research Analyses (OAR)
Holloman Air Force Base, New Mexico 88330
Attention: RRRD

Air Force Missile Test Center (1)
Patrick Air Force Base, Florida
Attention: L. J. Ullian

Air Force Systems Division (1)
Air Force Unit Post Office
Los Angeles, California 90045
Attention: Colonel Clark, Technical Data Center

Arnold Engineering Development Center (1)
Arnold Air Force Station
Tullahoma, Tennessee
Attention: Dr. H. K. Doetsch

Bureau of Naval Weapons (1)
Department of the Navy
Washington, D. C.
Attention: J. Kay, RTMS-41

Defense Documentation Center Headquarters (1)
Cameron Station, Building 5
5010 Duke Street
Alexandria, Virginia 22314
Attention: TISIA

Headquarters, U. S. Air Force (1)
Washington, D. C.
Attention: Colonel C. K. Stambaugh, AFRST

Picatinny Arsenal (1)
Dover, New Jersey 07801
Attention: I. Forsten, Chief
Liquid Propulsion Laboratory, SMUPA-DL

Air Force Rocket Propulsion Laboratory (1)
Research and Technology Division
Air Force Systems Command
Edwards, California 93523
Attention: RPF, Mr. H. Main

Union Carbide Corporation (1)
Nuclear Division
ORGDP Records Department, P. O. Box P
Oak Ridge, Tennessee 37830
Attention: A. P. Huber
Oak Ridge Gaseous Diffusion Plant

U. S. Army Missile Command (1)
Redstone Arsenal
Alabama 35809
Attention: Dr. Walter Wharton

U. S. Naval Ordnance Test Station (1)
China Lake
California 93557
Attention: Chief, Missile Propulsion Division
Code 4562

Chemical Propulsion Information Agency
Applied Physics Laboratory
8621 Georgia Avenue
Silver Spring, Maryland 20910
Attention: Neil Safeer

INDUSTRY CONTRACTORS

Aerojet-General Corporation (1)
P. O. Box 296
Azusa, California 91703
Attention: L. F. Kohrs

Aerojet-General Corporation (1)
P. O. Box 1947
Technical Library, Building 2015, Dept. 2410
Sacramento, California 95809
Attention: R. Stiff

Aeronutronic (1)
Philco Corporation
Ford Road
Newport Beach, California 92663
Attention: Librarian

Aerospace Corporation (1)
2400 East El Segundo Boulevard
P. O. Box 95085
Los Angeles, California 90045
Attention: John G. Wilder
MS-2293, Propulsion Department

Arthur D. Little, Incorporated (1)
20 Acorn Park
Cambridge, Massachusetts 02140
Attention: E. Karl Bastress

Astropower Laboratory (1)
Douglas Aircraft Company
2121 Paularino
Newport Beach, California 92663
Attention: Dr. George Moc, Director, Research

Astrosystems International, Incorporated (1)
1275 Bloomfield Avenue
Fairfield, New Jersey 07007
Attention: A. Mendenhall

Atlantic Research Corporation (1)
Edsall Road and Shirley Highway
Alexandria, Virginia 22314
Attention: A. Scurlock

Beech Aircraft Corporation (1)
Boulder Division
P. O. Box 631
Boulder, Colorado
Attention: J. H. Rodgers

Bell Aerosystems Company (1)
P. O. Box 1
Buffalo, New York 14240
Attention: W. M. Smith

Bendix Systems Division (1)
Bendix Corporation
3300 Plymouth Road
Ann Arbor, Michigan
Attention: John M. Brueger

Boeing Company (1)
P. O. Box 3707
Seattle, Washington 98124
Attention: J. D. Alexander

Missile Division (1)
Chrysler Corporation
P. O. Box 2628
Detroit, Michigan 48231
Attention: John Gates

Wright Aeronautical Division (1)
Curtiss-Wright Corporation
Wood-Ridge, New Jersey 07075
Attention: G. Kelley

Missile and Space Systems Division (1)
Douglas Aircraft Company, Incorporated
3000 Ocean Park Boulevard
Santa Monica, California 90406
Attention: R. W. Hallet, Chief Engineer
Advanced Space Technology

Aircraft Missiles Division (1)
Fairchild Hiller Corporation
Hagerstown, Maryland
Attention: J. S. Kerr

General Dynamics/Astronautics (1)
Library & Information Services (128-00)
P. O. Box 1128
San Diego, California 92112
Attention: Frank Dore

Re-Entry Systems Department
General Electric Company
3198 Chestnut Street
Philadelphia, Pennsylvania 19101
Attention: F. E. Schultz

Advanced Engine & Technology Department (1)
General Electric Company
Cincinnati, Ohio 45215
Attention: D. Suichu

Grumman Aircraft Engineering Corporation (1)
Bethpage, Long Island
New York
Attention: Joseph Gavin

Ling-Temco-Vought Corporation
Astronautics
P. O. Box 5907
Dallas, Texas 75222
Attention: Warren C. Trent

Lockheed California Company
2555 North Hollywood Way
Burbank, California 91503
Attention: G. D. Brewer

Lockheed Missiles and Space Company (1)
P. O. Box 504
Sunnyvale, California 94088
Attention: Y. C. Lee
Technical Information Center

Lockheed Propulsion Company (1)
P. O. Box 111
Redlands, California 92374
Attention: H. L. Thackwell

The Marquardt Corporation (1)
16555 Saticoy Street
Van Nuys, California 91409
Attention: Warren P. Boardman, Jr.

Baltimore Division (1)
Martin Marietta Corporation
Baltimore, Maryland 21203
Attention: John Calathes (3214)

Denver Division (1)
Martin Marietta Corporation
P. O. Box 179
Denver, Colorado 80201
Attention: J. D. Goodlette (A-241)

McDonnell Aircraft Corporation
P. O. Box 516
Municipal Airport
St. Louis, Missouri 63166
Attention: R. A. Herzmark

Space & Information Systems Division (1)
North American Aviation, Incorporated
12214 Lakewood Boulevard
Downey, California 90241
Attention: H. Storms

Rocketdyne (Library 586-306) (1)
North American Aviation, Incorporated
6633 Canoga Avenue
Canoga Park, California 91304
Attention: E. B. Monteath

Northrop Space Laboratories (1)
3401 West Broadway
Hawthorne, California
Attention: Dr. William Howard

Astro-Electronics Division (1)
Radio Corporation of America
Princeton, New Jersey 08540
Attention: S. Fairweather

Reaction Motors Division (1)
Thiokol Chemical Corporation
Denville, New Jersey 07832
Attention: Arthur Sherman

Republic Aviation Corporation
Farmingdale Long Island, New York
Attention: Dr. William O'Donnell

Space General Corporation (1)
9200 East Flair Avenue
El Monte, California 91734
Attention: C. E. Roth

Stanford Research Institute (1)
333 Ravenswood Avenue
Menlo Park, California 94025
Attention: Lionel Dickinson

TRW Systems Group (1)
TRW Incorporated
One Space Park
Redondo Beach, California 90278
Attention: G. W. Elverum

TAPCO Division (1)
TRW, Incorporated
23555 Euclid Avenue
Cleveland, Ohio 44117
Attention: P. T. Angell

Thiokol Chemical Corporation (1)
Huntsville Division
Huntsville, Alabama
Attention: John Goodloe

Research Laboratories (1)
United Aircrait Corporation
400 Main Street
East Hartford, Connecticut 06108
Attention: Erle Martin

United Technology Center (1)
587 Methilda Avenue
P. O. Box 358
Sunnyvale, California 94088
Attention: B. Adelman

Aerospace Operations (1)
Walter Kidde and Company, Incorporated
567 Main Street
Belleville, New Jersey 07109
Attention: R. J. Hanville
Director of Research Engineering

Florida Research and Development (1)
Pratt and Whitney Aircraft
United Aircraft Corporation
P. O. Box 2691
West Palm Beach, Florida 33402
Attention: R. J. Coar

Rocket Research Corporation (1)
520 South Portland Street
Seattle, Washington 98108
Attention: Foy McCullough, Jr.